



## 저작자표시-비영리 2.0 대한민국

이용자는 아래의 조건을 따르는 경우에 한하여 자유롭게

- 이 저작물을 복제, 배포, 전송, 전시, 공연 및 방송할 수 있습니다.
- 이차적 저작물을 작성할 수 있습니다.

다음과 같은 조건을 따라야 합니다:



저작자표시. 귀하는 원저작자를 표시하여야 합니다.



비영리. 귀하는 이 저작물을 영리 목적으로 이용할 수 없습니다.

- 귀하는, 이 저작물의 재이용이나 배포의 경우, 이 저작물에 적용된 이용허락조건을 명확하게 나타내어야 합니다.
- 저작권자로부터 별도의 허가를 받으면 이러한 조건들은 적용되지 않습니다.

저작권법에 따른 이용자의 권리는 위의 내용에 의하여 영향을 받지 않습니다.

이것은 [이용허락규약\(Legal Code\)](#)을 이해하기 쉽게 요약한 것입니다.

[Disclaimer](#) 

**February 2015**

**Ph.D. Dissertation**

**Antimicrobial and Anti-inflammatory  
Activities and Mechanism of Action of  
Cathelicidin-derived Synthetic  
Antimicrobial Peptides**

**Graduate School of Chosun University**

**Department of Bio-Materials**

**Binu Jacob**

# **Antimicrobial and Anti-inflammatory Activities and Mechanism of Action of Cathelicidin-derived Synthetic Antimicrobial Peptides**

카텔리시딘 유래 합성 항균 펩타이드의 항균활성,  
항-염증 활성 및 작용 기작에 관한 연구

February 25, 2015

**Graduate School of Chosun University**

**Department of Bio-Materials**

**Binu Jacob**

# **Antimicrobial and Anti-inflammatory Activities and Mechanism of Action of Cathelicidin-derived Synthetic Antimicrobial Peptides**

**Advisor: Prof. Song Yub Shin**

*This dissertation is submitted to the Graduate School of  
Chosun University in partial fulfillment of the requirements  
for the degree of Doctor of Philosophy in Science*


**October 2014**

**Graduate School of Chosun University**

**Department of Bio-Materials**

**Binu Jacob**

**Binu Jacob's Ph.D. Dissertation has certified.**

Chairman (Chosun Univ.) : Prof. Il-Seon Park.....

Member (Chosun Univ.) : Prof. Seung Joo Cho.....

Member (Chosun Univ.) : Prof. Sung Haeng Lee.....

Member (Chosun Univ.) : Prof. Song Yub Shin.....

Member (Chonnam Univ.) : Prof. Chul Won Lee.....

December 2014

**Graduate School of Chosun University**

## CONTENTS

<b>CONTENTS</b> .....	i
<b>LIST OF TABLES</b> .....	iv
<b>LIST OF FIGURES</b> .....	v
<b>ABSTRACT (KOREAN)</b> .....	vii
<b>ABSTRACT (ENGLISH)</b> .....	xi
<b>PART I . Short KR-12 analogs designed from human cathelicidin LL-37 possessing both antimicrobial and antiendotoxic activities without mammalian cell toxicity</b> ...1	
<b>1. INTRODUCTION</b> .....	2
<b>2. MATERIALS AND METHODS</b> .....	5
<b>3. RESULTS AND DISCUSSION</b> .....	11
3.1. Peptide Design and Synthesis.....	11
3.2. Secondary Structure Studies using CD Spectroscopy .....	12
3.3. Antimicrobial (MIC) and Hemolytic (MHC) Activities.....	12
3.4. Therapeutic Index (TI).....	13
3.5. Anti-MRSA Activity.....	13
3.6. Cytotoxicity toward RAW264.7 cells.....	14
3.7. Anti-LPS activity.....	14
<b>4. CONCLUSION</b> .....	17

**5. REFERENCES.....27**

**PART II. Bacterial killing mechanism of sheep myeloid antimicrobial peptide-18 (SMAP-18) and its Trp-substituted analog with improved cell selectivity and reduced mammalian cell toxicity.....31**

**1. INTRODUCCION.....32**

**2. MATERIALS AND METHODS.....34**

**3. RESULTS ..... 41**

3.1 Antimicrobial and Hemolytic Activities.....41

3.2 Cytotoxicity against Mammalian Cells.....41

3.3 Dye Leakage from Model Membranes.....42

3.4 Membrane Depolarization.....42

3.5 Evaluation of Outer Membrane Permeability (NPN uptake)....43

3.6 Evaluation of Inner Membrane Permeability (ONPG hydrolysis)43

3.7 Time-kill Kinetics.....44

3.8 Confocal Laser Scanning Microscopy.....44

**4. DISCUSSION.....46**

**5. REFERENCES..... 60**

**PART III. Enantiomer and Diastereomers of sheep myeloid antimicrobial peptide-28 (SMAP-28) have improved activity and different membrane interaction...65**

**1. INTRODUCTION.....66**

**2. MATERIALS AND METHODS.....69**

**3. RESULTS.....75**

    3.1 Design and Synthesis of Peptides .....75

    3.2 Hydrophobicity of Peptides.....76

    3.3 Secondary Structure Studies by CD Spectroscopy.....76

    3.4 Antimicrobial and Hemolytic Activities.....77

    3.5 Cell Selectivity (Therapeutic Index).....78

    3.6 Cytotoxicity against RAW264.7 Cells.....78

    3.7 Anti-inflammatory Activity.....78

    3.8 Membrane Interaction.....79

    3.9 DNA Binding Activity.....80

    3.10 Antimicrobial activity by Agar Diffusion Assay.....80

    3.11 Time-killing Kinetics.....80

**4. DISCUSSION.....81**

**5. REFERENCES.....96**

**ACKNOWLEDGEMENTS.....100**



## LIST OF TABLES

### PART I

Table 1. Amino acid sequences and physicochemical properties of KR-12 and its analogs used for comparison.....	18
Table 2. Antimicrobial activity of KR-12 and its analogs.....	19
Table 3. Cell specificity (therapeutic index) and antiendotoxic activity of KR-12 and its analogs.....	20

### PART II

Table 1. Amino acid sequences, calculated and observed molecular masses of SMAP-29, SMAP-18 and its analog.....	50
Table 2. Antimicrobial and hemolytic activities and cell selectivity (therapeutic index) of SMAP-29, SMAP-18 and SMAP-18-W.....	51

### PART III

Table 1. Amino acid sequences and physicochemical properties of SMAP-29 and SMAP-18 and Enantiomers and diastereomers.....	85
Table 2. Antimicrobial activity of SMAP-29, SMAP-18, their enantiomers and diastereomers.....	86
Table 3. Antimicrobial activity of the peptides against MRSA.....	87
Table 4. Cell specificity (therapeutic index) of SMAP-29, SMAP-18, their enantiomers and diastereomers.....	88

## LIST OF FIGURES

### PART I

Figure 1. Helical wheel diagrams for KR-12 and its analogs .....	21
Figure 2. Circular dichroism (CD) spectra of the peptides .....	22
Figure 3. Concentration–response curves of hemolysis of KR-12 and its analogs against human red blood cells.....	23
Figure 4. Cytotoxicity of KR-12 and its analogs against macrophage-derived RAW264.7 cells.....	24
Figure 5. Inhibitory effects of KR-12 and its analogs on LPS-stimulated TNF- $\alpha$ production in RAW264.7 cells.....	25
Figure 6. Ability of the peptides to bind with LPS was evaluated by Limulus Amebocyte Lysate (LAL) Kinetic-QCL™ .....	26

### PART II

Figure 1. Concentration–response curves of percent hemolysis of SMAP-29, SMAP-18 and SMAP-18-W against human red blood cells.....	52
Figure 2. Cytotoxicity of SMAP-29, SMAP-18 and SMAP-18-W against three different types of mammalian cells.....	53
Figure 3. Peptide-induced calcein release from calcein-entrapped liposomes...54	
Figure 4. Membrane depolarization of <i>Staphylococcus aureus</i> by SMAP-29, SMAP-18 and SMAP-18-W.....	55
Figure 5. Peptide-mediated NPN uptake in <i>Escherichia coli</i> cells.....	56
Figure 6. Peptide-mediated inner membrane permeabilization of <i>E.coli</i> ML-35...57	

Figure 7. Time-kill kinetics of peptides on *E.coli* and *Staphylococcus aureus*...58

Figure 8. Confocal laser scanning microscopy of *Escherichia coli* or  
*Staphylococcus aureus* treated with FITC-labeled peptides.....59

**PART III**

Figure 1. Circular dichroism spectra of the peptides .....89

Figure 2. Peptides induced hemolysis and cytotoxicity.....90

Figure 3. Peptide inhibition of LPS induced cytokines in RAW 264.7 cells.....91

Figure 4. Peptide induced (A) membrane depolarization as measured by release of  
Disc3 (5) dye from membrane, (B) leak of calcein dye from bacterial  
membrane mimicking liposomes.....92

Figure 5. SMAP-18L and SMAP-18D – DNA binding affinity.....93

Figure 6. MIC by agar diffusion method against *E. coli* for SMAP-18L, SMAP-  
18D, SMAP-18DA.....94

Figure 7. Killing Kinetics of SMAP-18L and SMAP-18D against *E. coli*.....95

## 초 록

### 카텔리시딘 유래 및 모델 항균펩타이드의 세포선택성, 작용기작 및 항염증활성

자콥 비누

지도교수: 신송엽, Ph.D.

생물신소재학과

조선대학교 대학원

#### Part I

KR-12 (LL-37의 18–29잔기)는 항균활성을 가지는 사람의 캐더라시딘 LL-37으로부터 유래된 가장 짧은 항균 펩타이드(antimicrobial peptide: AMP)이다. 포유류 세포에 대해 활성을 가지지 않고 항균활성과 항-내독소활성(LPS-endotoxic activity)을 가지는 알파-헬릭스 구조의 짧은 항균 펩타이드(AMP)를 얻기 위해, KR-12 유사체를 설계하고 합성하였다. KR-12 유사체중에 가장 소수성이 강한 KR-12-a5와 KR-12-a6는 LPS-자극 tumor necrosis factor- $\alpha$  (TNF- $\alpha$ )생산을 강하게 억제하였으며, 높은 LPS-결합활성을 보였다. 펩타이드의 항균활성은 전하(charge)와는 무관하고, LPS-중성화능력(LPS-neutralizing ability)은 펩타이드의 소수성과 순수 양전하(net positive charge)의 균형이 필요하다는 것을 알았다. KR-12 유사체중에 KR-12-a2, KR-12-a3과 KR-12-a4는 세균과 적혈구세포간의 아주 높은 세포 특이성(cell specificity)을 나타내었다. KR-12-a5는 LL-37과 비교해서, 보다 강한 항-내독소 활성을

나타낸 반면에, 가장 낮은 세포 특이성을 나타내었다. 또한 KR-12-a2, KR-12-a3, KR-12-a4 및 KR-12-a5는 메티실린 저항성-*Staphylococcus aureus* (MRSA)에 대하여 4 $\mu$ M의 MIC값을 가지는 강한 항균활성을 나타내었다. 정리하면, 따라서 새로이 설계 합성된 몇 종 KR-12유사체는 미래의 새로운 항균 및 항-염증제로서 잠재성을 가지고 있었다.

## Part II

Sheep myeloid antimicrobial peptide-29 (SMAP-29)와 비교하여, 세포 선택성(cell selectivity)를 증가시키고, 포유류 세포에 대한 독성을 감소시킨 짧은 항균 펩타이드를 개발하고, 항균작용기작을 규명하기 위해, SMAP-29의 N-말단의 18잔기로 이루어진 펩타이드(SMAP-18) 및 트립토판(Trp)-치환유사체 (SMAP-18-W)를 합성하였다. 용혈활성의 감소와 항균활성의 유지로 인하여, SMAP-18와 SMAP-18-W는 SMAP-29보다 높은 세포 선택성을 나타내었다. SMAP-18와 SMAP-18-W는 100 $\mu$ M에서도 RAW 264.7, NIH-3T3 및 HeLa세포와 같은 포유류 세포에 대해 세포독성을 전혀 나타내지 않았다. 이 결과는 SMAP-18와 SMAP-18-W가 미래의 새로운 치료용 항균제로서 잠재성을 가진다는 것을 시사하였다. SMAP-29와 달리, SMAP-18와 SMAP-18-W는 세균막 모방 리포솜으로부터 dye유출, N-phenyl-1-naphthylamine (NPN) 흡수(uptake) 및 o-nitrophenyl- $\beta$ -galactoside(ONPG)의 가수분해능력이 비교적 약함을 보였다. SMAP-29과 비슷하게, SMAP-18-W는 *Staphylococcus aureus*에 있어서 2 $\times$ MIC에서 약80%의 막탈분극(membrane depolarization)을 일으켰다. 반면에 SMAP-18은 4 $\times$ MIC에서도 막탈분극을 일으키지 않았다. Confocal laser scanning microscopy실험에서, SMAP-18은 비막파괴적 양상(non-membrane disruptive manner)으로 세포막을 가로질러 이동하였다. 반면에 SMAP-29는 SMAP-18-W는 세균막을 통과하지 못하였다. 정리하면, SMAP-29은 지질 이중막의 파괴함으로서, SMAP-18-W는

세균세포막에 구멍이나 이온채널을 형성함으로써 세균을 죽이고, SMAP-18은 세포내 표적메카니즘(intracellular-targeting mechanism)에 의하여, 세균을 죽이는 메커니즘이라는 사실이 제안되었다.

### Part III

Sheep myeloid antimicrobial peptide-29 (SMAP-29)는 강한 항균작용을 나타내지만 동시에 독성을 가진 항균 펩타이드 이다. SMAP-29는 3개의 이소루이신 (Ile)을 포함하고 있는 소수성 C-말단 (19-28잔기)은 용혈활성과 독성을 담당하고 있다. SMAP-29의 C-말단 소수성 영역의 막결합성을 조사하기 위해 D-enantiomer (SMAP-29D) D-allo-이소루이신을 포함하는 diastereomer(SMAP-29DA)를 조제하였다. 또한 SMAP-29의 세포 선택성(cell selectivity) 및 LPS중화활성을 증진시키기 위해 SMAP-29의 1-18 잔기는 L-형 아미노산, 19-28 잔기는 D-형 아미노산으로 이루어진 2개의 이성질체 (SMAP-29HD와SMAP-29HDA)를 합성하였다. SMAP-18이라고 명명된 SMAP-29의 비용혈활성N-말단(1-18잔기)는 세포내 표적(intracellular target)을 가진다. 세포내 키랄작용(chiral interaction)을 찾아내고, 세포투과 효율(membrane penetrating efficiency)를 조사하기 위해 펩타이드의 SMAP-18의 D-enantiomer (SMAP-18D) 와 diastereomer (SMAP-18DA)를 제조하였다. SMAP-29HD와 SMAP-29HDA를 제외한 모든 펩타이드는 SDS 또는 LPS존재하에서 전형적인 알파-헤릭스 구조를 나타내었다. SMAP-29DA, SMAP-29HD 와SMAP-29HDA는 SMAP-29의 L- 및 D-enantiomer 에 비하여 비교적 낮은 소수성 및 용혈활성을 나타내었으며, 수십 배의 치료지수(therapeutic index)의 증가를 보였다. SMAP-29 펩타이드들은 RAW264.7세포에 있어서 LPS-유도성 NO, TNF- $\alpha$ , IL-6 및 MCP-1의 생산을 강력히 저해하였다. 그러나 SMAP-18 펩타이드들은 그렇지 못하였다. SMAP-29HD 및 SMAP-29HDA는 RAW264.7세포에 덜 약한 독성을 나타내었다.

SMAP-29 펩타이드들은 *Staphylococcus aureus*에 대한 막탈분극(membrane depolarization)을 강하게 유도하였지만 SMAP-18은 막탈분극을 일으키지 않았다. SMAP-29L, SMAP-29D와 SMAP-29DA는 세균막 모방 리포솜으로부터 calcein dye를 쉽고 빠르게 방출시켰지만, SMAP-29HD와SMAP-29HDA는 리포솜으로부터 충분한 방출을 일으키는데 좀 많은 시간 소요되었다. Broth dilution assay에 있어서 SMAP-18D 와 SMAP-18DA는 SMAP-18에 비해 다섯 개 균주에 대해 4배에서 8배의 높은 항균활성을 나타내었다. Agar diffusion assay에 있어서, SMAP-18L은 작지만 선명한 투명 존(clear zone)을 나타내었으며, SMAP-18D와SMAP-18DA는 넓지만 흐린 투명 존을 나타내었다. SMAP-18L and SMAP-18D은 2 $\mu$ M농도에서 세균의 플라스미드DNA와 효과적으로 결합하였다. SMAP-18L은 SMAP-18D보다 빠르게 *E. coli*를 죽였다. SMAP-29 와 SMAP-18 펩타이드는 3개의 메티실린-저항성*Staphylococcus aureus* (MRSA)에 대해 좋은 항균활성을 나타내었다.

## ABSTRACT

### **Antimicrobial and Anti-inflammatory Activities and Mechanism of Action of Cathelicidin-derived Synthetic Antimicrobial Peptides**

Binu Jacob

Advisor: Prof. Song Yub Shin

Department of Bio-Materials

Graduate School of Chosun University

#### **PART I**

KR-12 (residues 18-29 of LL-37) was known to be the smallest peptide of human cathelicidin LL-37 possessing antimicrobial activity. In order to optimize  $\alpha$ -helical short antimicrobial peptides having both antimicrobial and antiendotoxic activities without mammalian cell toxicity, we designed and synthesized a series of KR-12 analogs. Highest hydrophobic analogs KR-12-a5 and KR-12-a6 displayed greater inhibition of LPS-stimulated TNF- $\alpha$  production and higher LPS-binding activity. We have observed that antimicrobial activity is independent of charge but LPS neutralization requires a balance of hydrophobicity and net positive charge. Among



KR-12 analogs, KR-12-a2, KR-12-a3 and KR-12-a4 showed much higher cell specificity for bacteria over erythrocytes and retained antiendotoxic activity, relative to parental LL-37. KR-12-a5 displayed the strongest antiendotoxic activity, whereas almost similar cell specificity as compared to LL-37. Also, these KR-12 analogs (KR-12-a2, KR-12-a3, KR-12-a4 and KR-12-a5) exhibited potent antimicrobial activity (MIC: 4  $\mu$ M) against methicillin-resistant *Staphylococcus aureus*. Taken together, these KR-12 analogs have the potential for future development as novel class of antimicrobial and anti-inflammatory therapeutic agents.

## **PART II**

To develop short antimicrobial peptide (AMPs) with improved cell selectivity and reduced mammalian cell toxicity compared to sheep myeloid antimicrobial peptide-29 (SMAP-29) and elucidate the possible mechanisms responsible for their antimicrobial action, we synthesized an N-terminal 18-residues peptide amide (SMAP-18) from SMAP-29 and its Trp-substituted analog (SMAP-18-W). Due to their reduced hemolytic activity and retained antimicrobial activity, SMAP-18 and SMAP-18-W showed higher cell selectivity than SMAP-29. In addition, SMAP-18 and SMAP-18-W had no cytotoxicity against three different mammalian cells such as RAW 264.7, NIH-3T3 and HeLa cells even at 100  $\mu$ M. These results suggest that SMAP-18 and SMAP-18-W has potential for future development as novel therapeutic antimicrobial agent. Unlike SMAP-29, SMAP-18 and SMAP-18-W showed relatively weak ability to induce dye leakage from bacterial membrane-mimicking liposomes, N-phenyl-1-naphthylamine (NPN) uptake and o-nitrophenyl- $\beta$ -galactoside (ONPG) hydrolysis. Similar to SMAP-29, SMAP-18-W led to a significant membrane depolarization (>80%) against *Staphylococcus aureus* at 2  $\times$  MIC. In contrast, SMAP-18 didn't cause any membrane depolarization even at 4  $\times$  MIC. In confocal laser scanning microscopy, we observed translocation of SMAP-18 across the membrane in a non-membrane disruptive manner. SMAP-29 and

SMAP-18-W was unable to translocate the bacterial membrane. Collectively, we propose here that SMAP-29 and SMAP-18-W kill microorganisms by disrupting/perturbing the lipid bilayer and forming pore/ion channels on bacterial cell membranes, respectively. In contrast, SMAP-18 may kill bacteria via intracellular-targeting mechanism.

### PART III

Sheep myeloid antimicrobial peptide-29 (SMAP-29) is a potent but equally cytotoxic antimicrobial peptide. Its highly hydrophobic C-terminal region (19-29 residues) containing three isoleucines is responsible for hemolytic and cytotoxic activities. To study the membrane interaction of this hydrophobic region, D-enantiomer (SMAP-29D), and diastereomer (SMAP-29DA) containing D-allo-isoleucines had prepared. To improve cell selectivity and LPS neutralization ability of SMAP-29, 2 isomers consist of L-form (1-18 residues) and D-form (19-28 residues) segments were also synthesized (SMAP-29HD and SMAP-29HDA). The non-hemolytic N-terminal region (SMAP-18, 1-18 residues) is having an intracellular target. We had prepared D-enantiomer (SMAP-18D) and diastereomer (SMAP-18DA) of SMAP-18 to probe the cytoplasmic chiral interaction and to study the membrane penetrating efficiency of enantiomeric peptides. Except SMAP-29HD and SMAP-29HDA, all peptides showed a typical  $\alpha$ -helical conformation in the presence of SDS or LPS. SMAP-29DA, SMAP-29HD and SMAP-29HDA had significantly lesser relative hydrophobicity, hemolytic activity, and several fold increase in therapeutic index than the corresponding L- and D-enantiomer of SMAP-29. SMAP-29 peptides but not SMAP-18 peptides showed a powerful inhibition of LPS-induced production of NO, TNF- $\alpha$ , IL-6 and MCP-1 in RAW264.7 cells. SMAP-29HD and SMAP-29HDA were less cytotoxic to RAW264.7 cells. SMAP-29 peptides showed instant membrane depolarization against *Staphylococcus aureus*, but SMAP-18 peptides did not induce membrane depolarization. SMAP-29L, SMAP-29D and SMAP-

29DA readily released dye from bacterial membrane mimicking liposomes. SMAP-29HD and SMAP-29HDA took longer time to reach full release of dye from liposomes. SMAP-18D and SMAP-18DA showed 4- or 8-fold higher antimicrobial activity against five bacteria in broth dilution assay. In agar diffusion assay, SMAP-18L had smaller but distinct clear zone but SMAP-18D and SMAP-18DA had border but blurred clear zone. Both SMAP-18L and SMAP-18D peptides binds with bacterial plasmid DNA at  $2\mu\text{M}$ . SMAP-18L killed *E. coli* faster than SMAP-18D. Both SMAP-29 and SMAP-18 peptides showed good activity against 3 MRSA strains.

## **PART I**

**Short KR-12 analogs designed from human cathelicidin LL-37 possessing both antimicrobial and antiendotoxic activities without mammalian cell toxicity**

# 1. Introduction

LPS (lipopolysaccharide), also known as endotoxin, is a major constituent of the outer membrane of Gram-negative bacteria [1,2]. The antibiotic therapy against Gram-negative bacterial infections is often accompanied by the release of LPS [1,2]. LPS is recognized as a key molecule in the pathogenesis of septic shock syndromes associated with serious Gram-negative bacterial infections [1,2]. Although the exact mechanism is not yet well understood, upon its release, LPS is recognized by mononuclear phagocytes (monocytes and macrophages), and it activates them. This enhances their phagocytic activity and significantly raises the secretion level of proinflammatory cytokines, such as tumor necrosis factor- $\alpha$  (TNF- $\alpha$ ), interleukin-6 (IL-6), and others [3-6]. However, an unbalanced systemic secretion of these cytokines can rapidly give rise to septic shock syndrome, frequently resulting in death [3-6]. The neutralization of LPS-mediated toxic injury has been considered for a long time to be as possible therapeutic target in patients.

Antimicrobial peptides (AMPs) are components of the innate immune system and have been identified in almost all living organisms, ranging from plants to insects to mammals, including humans [7,8]. AMPs are capable of targeting bacteria, fungi, and enveloped viruses and are considered potential alternatives to conventional antibiotics, as they physically disrupt the bacterial membranes, leading to membrane lysis and eventually cell death [7,8]. Human cathelicidin LL-37 is a 37 residue long cationic and amphipathic  $\alpha$ -helical AMP [9]. Besides direct antimicrobial action, LL-37 is known to be effective in binding to and neutralizing LPS and consequently has considerable potential in the treatment of endotoxin shock and sepsis associated with Gram-negative bacterial infections [10-14]. These properties make LL-37 as an attractive therapeutic

agent for Gram-negative bacterial infection and inflammatory disease [10-14]. Even though LL-37 has potent antimicrobial and LPS-neutralizing activities, it causes a significant hemolysis toward human red blood cells [15]. The length of LL-37 is too long to develop as a therapeutic agent for Gram-negative bacterial infection and inflammatory disease. Short AMPs attract attention due to the potentially lower cost of production.

For this reason, we used a 12-meric short KR-12peptide (residues18-29 of LL-37) identified as the smallest region of LL-37 possessing antimicrobial activity [16], to optimize short AMPs having cell specificity and antiendotoxic activity. We designed and synthesized a series of amino acid-substituted analogs from the  $\alpha$ -helical wheel diagram of KR-12. The cell selectivity of peptides was investigated by examining their antimicrobial activity against Gram-positive and Gram-negative bacterial strains, and their hemolytic activity against human red blood cells. The LPS-neutralizing activity of peptides was evaluated by examining their inhibition of TNF- $\alpha$ production in LPS-stimulated mouse macrophage RAW264.7 cells. The ability of KR-12 and its analogs to bind LPS were assessed using chromogenic *Limulus* amoebocyte lysate (LAL) assay. The secondary structure of the peptides in the presence of LPS was investigated by circular dichroism(CD) spectroscopy. Our results will help in the design of novel short  $\alpha$ -helical AMPs having both antimicrobial and antiendotoxic activities without mammalian cell toxicity. LPS (lipopolysaccharide), also known as endotoxin, is a major constituent of the outer membrane of Gram-negative bacteria [1,2]. The antibiotic therapy against Gram-negative bacterial infections is often accompanied by the release of LPS [1,2]. LPS is recognized as a key molecule in the pathogenesis of septic shock syndromes associated with serious Gram-negative bacterial infections [1,2]. Although

the exact mechanism is not yet well understood, upon its release, LPS is recognized by mononuclear phagocytes (monocytes and macrophages), and it activates them. This enhances their phagocytic activity and significantly raises the secretion level of proinflammatory cytokines, such as tumor necrosis factor- $\alpha$  (TNF- $\alpha$ ), interleukin-6 (IL-6), and others [3-6]. However, an unbalanced systemic secretion of these cytokines can rapidly give rise to septic shock syndrome, frequently resulting in death [3-6]. The neutralization of LPS-mediated toxic injury has been considered for a long time to be as possible therapeutic target in patients.

## 2. Materials and Methods

### 2.1. Materials

Fmoc (9-fluorenylmethoxycarbonyl) amino acids and Fmoc amino acid-Wang resins were purchased from Calbiochem-Novabiochem (La Jolla, CA). Other reagents used for peptide synthesis including trifluoroacetic acid (TFA; sigma), piperidine (Merck), dicyclohexylcarbodiimide (DCC; Fluka), N-hydroxybenzotriazole hydrate (HOBT; Aldrich) and dimethylformamide (DMF, peptide synthesis grade; Biolab). Lipopolysaccharide (LPS from *Escherichia coli* O111:B4), and 3-(4,5-dimethylthiazol-2-yl)-2,5-diphenyl-2H-tetrazolium bromide (MTT) were obtained from Sigma Chemical Co (St. Louis, MO). DMEM and fetal bovine serum (FBS) were purchased from HyClone (SeouLin, Bioscience, Korea). RAW 264.7 cells were procured from American Type culture Collection (Bethesda, MD). All other reagents were of analytical grade. The buffers were prepared in double glass-distilled water

### 2.2 Peptide Synthesis

Peptides listed in Table 1 were prepared by the standard Fmoc-based solid-phase synthesis technique on rink amide-4-methylbenzhydrylamine resin (0.54 mmol/g). DCC (dicyclohexylcarbodiimide) and HOBT (N-hydroxybenzotriazole) were used as coupling reagents, and a 10-fold excess of Fmoc-amino acids was added during every coupling cycle. After cleavage and deprotection with a mixture of trifluoroacetic acid/water/thioanisole/phenol/ethanedithiol/triisopropylsilane (81.5 : 5 : 5 : 5 : 2.5:1, v/v/v/v/v) for 2 h at room temperature, the crude peptide was repeatedly extracted with diethyl ether and purified by RP-HPLC (reverse-phase high-performance liquid



chromatography) on a preparative Vydac C18 column (20 mm ×250 mm, 300 Å, 15-mm particle size) using an appropriate 0–90% water/acetonitrile gradient in the presence of 0.05% trifluoroacetic acid. The final purity of the peptides (>95%) was assessed by RP-HPLC on an analytical Vydac C18 column (4.6×250 mm, 300 Å, 5-mm particle size). The success of the synthesis of the peptide was confirmed by analysis using a matrix-assisted laser desorption/ionization, time-of-flight (MALDI-TOF) mass spectrometry (Shimadzu, Japan)(Table 1).

### 2.3 Antimicrobial Activity (MIC)

The antimicrobial activity of the peptides against three Gram-positive bacterial strains, three Gram-negative bacterial strains and three MRSA strains was examined by using the broth microdilution method in sterile 96-well plates. Aliquots (100 µl) of a bacterial suspension at  $2 \times 10^6$  colony-forming units (CFU)/mL in 1% peptone were added to 100 µl of the peptide solution (serial 2-fold dilutions in 1% peptone). After incubation for 18–20 h at 37°C, bacterial growth inhibition was determined by measuring the absorbance at 600 nm with a Microplate Autoreader EL 800 (Bio-Tek Instruments, VT). The minimal inhibitory concentration (MIC) was defined as the minimum peptide concentration that inhibited bacteria growth. Three types of gram-positive bacteria (*Bacillus subtilis* [KCTC 3068], *Staphylococcus epidermidis* [KCTC 1917] and *Staphylococcus aureus* [KCTC 1621]) and three types of gram-negative bacteria (*Escherichia coli* [KCTC 1682], *Pseudomonas aeruginosa* [KCTC 1637] and *Salmonella typhimurium* [KCTC 1926]) were procured from the Korean Collection for Type Cultures (KCTC) at the Korea Research Institute of Bioscience and Biotechnology (KRIBB). Three methicillin-resistant *Staphylococcus aureus* (MRSA) (CCARM 3089,

CCARM 3090 and CCARM 3095) were obtained from the Culture Collection of Antibiotic-Resistant Microbes (CCARM) at Seoul Women's University (Seoul, Korea).

## 2.4 Hemolytic Activity

Fresh human red blood cells (hRBCs) were centrifuged, washed three times with phosphate-buffered saline (PBS) (35 mM phosphate buffer, 0.15 M NaCl, pH 7.4), dispensed into 96-well plates as 100  $\mu$ l of 4% (w/v) hRBC in PBS, and 100  $\mu$ l of peptide solution was added to each well. Plates were incubated for 1 h at 37 °C, then centrifuged at 1000  $\times$  g for 5 min. Samples (100  $\mu$ l) of supernatant were transferred to 96-well plates and hemoglobin release was monitored by measuring absorbance at 414 nm. Zero hemolysis was determined in PBS ( $A_{\text{PBS}}$ ) and 100% hemolysis was determined in 0.1% (v/v) Triton X-100 ( $A_{\text{triton}}$ ). The hemolysis percentage was calculated as: % hemolysis =  $100 \times [(A_{\text{sample}} - A_{\text{PBS}}) / (A_{\text{triton}} - A_{\text{PBS}})]$

## 2.5 Circular Dichroism (CD) Spectroscopy

The CD spectrum of the peptide was obtained with a Jasco J-715 CD spectrophotometer (Tokyo, Japan) at 25 °C using a fused quartz cell with a 1-mm path length over a wavelength range of 190–250 nm at 0.1 nm intervals (speed, 50 nm/min; response time, 0.5 s; bandwidth, 1 nm). CD spectra were collected and averaged over three scans. Samples were prepared by dissolving the peptide to a final concentration of 100  $\mu$ g/mL in 10mM sodium phosphate buffer (pH7.2) or 0.1% LPS. The mean residue ellipticity  $[\theta]$ , was given in degree  $\cdot \text{cm}^2 \cdot \text{dmol}^{-1}$ . The spectra were expressed as molar ellipticity  $[\theta]$  vs. wavelength. The fractional helical content  $f_{\alpha}$  of peptides in a helical conformation was calculated as follows:

$$\text{Fractional helical content } (f_a) = (\theta - \theta_{RC}) / (\theta_H - \theta_{RC}),$$

where  $\theta$  is observed ellipticity and  $\theta_{RC}$  and  $\theta_H$  are the limiting values for a completely random coil and a completely helical conformation, respectively. Here, we use the following values, both at 222 nm:  $\theta_{RC} = -1.5 \times 10^3 \text{ degree} \cdot \text{cm}^{-2} \cdot \text{dmol}^{-1}$  and  $\theta_H = -33.4 \times 10^3 \text{ degree} \cdot \text{cm}^{-2} \cdot \text{dmol}^{-1}$  [17].

## 2.6 Cell Culture

RAW 264.7 cells were purchased from the American Type Culture Collection (Manassas, VA) and cultured in DMEM supplemented with 10% fetal bovine serum and antibiotic-antimycotic solution (100 units/ml penicillin, 100 $\mu$ g/ml streptomycin and 25 $\mu$ g/ml amphotericin B) in 5% CO<sub>2</sub> at 37 °C. Cultures were passed every 2 to 3 days, and cells were detached by brief trypsin treatment, and visualized with an inverted microscope.

## 2.7 Cytotoxicity (MTT proliferation assay)

Cytotoxicity of peptides against RAW 264.7 cells was determined using the MTT assay. The cells were seeded on 96-well microplates at a density of  $2 \times 10^4$  cells/well in 150  $\mu$ l DMEM containing 10% fetal bovine serum. Plates were incubated for 24 h at 37 °C in 5% CO<sub>2</sub>. Peptide solutions (20  $\mu$ L) (serial 2-fold dilutions in DMEM) were added, and the plates further incubated for 2 days. Wells containing cells without peptides served as controls. Subsequently, 20  $\mu$ l MTT solution (5 mg/ml) was added in each well, and the plates were incubated for a further 4 h at 37°C. Precipitated MTT formazan was dissolved in 40  $\mu$ l of 20% (w/v) SDS containing 0.01 M HCl for 2h. Absorbance at 570

nm was measured using a microplate ELISA reader (Molecular Devices, Sunnyvale, CA). Cell survival was expressed as a percentage of the ratio of  $A_{570}$  of cells treated with peptide to that of cells only.

## **2.8 Assay for Evaluation of LPS-neutralizing Activity**

Cultured RAW264.7 macrophage cells at  $5 \times 10^5$  cells/well in 96-well plate were stimulated with *E. coli* LPS O111:B4 (20 ng/ml) in the presence (10 $\mu$ M) or absence of peptides. Cells stimulated with LPS alone and untreated cells were used for maximum and minimum tumor necrosis factor- $\alpha$  (TNF- $\alpha$ ) production in a given set of experiments. The cells were later incubated for 6 h at 37°C in an incubator. Afterward, samples of the medium from each treatment were collected. Concentrations TNF- $\alpha$  in the samples were evaluated using mouse enzyme-linked immunosorbent assay kits for TNF- $\alpha$  (R&D Systems, Minneapolis, MN, USA) according to the manufacturers' protocol, and data were presented in terms of percentage inhibition of LPS-induced cytokine production in the presence of these peptides.

## **2.9 Binding of Peptides to Endotoxin (LAL assay)**

The abilities of KR-12 and its analogs to bind LPS were assessed using a quantitative chromogenic Limulus amoebocyte lysate (LAL) with a QCL-1000 (Lonza 50-647U) kit. Experiments were carried out following the protocols recommended by the manufacturer. Peptides at concentrations of 0.25, 0.5, 1, 2.5, 5 and 10 $\mu$ M were incubated with 3.0 endotoxin units (EU) of LPS in non pyrogenic micro tubes at 37°C for 30 min to allow the binding of peptides to LPS. A total of 50 $\mu$ L of this mixture was then added to an equal volume of LAL reagent (50 $\mu$ L), and the mixture was further

incubated for 10 min, followed by the addition of 100  $\mu$ L of LAL chromogenic substrate (Ac-Ile-Ala-Arg-*p*-nitroaniline). The reaction was terminated by the addition of 37% sulphuric acid, and the yellow color that developed due to cleavage of the substrate was measured spectrophotometrically at 450 nm. The reduction of absorbance at 450 nm as a function of the peptide concentration is directly proportional to the inhibition of LPS by the peptide.

## 3. Results and Discussion

### 3.1 Peptide Design and Synthesis

In this study, we had systematically altered the net positive charge and hydrophobicity of the peptides to obtain the effective short AMPs having antimicrobial and antiendotoxic activities without mammalian cell toxicity. Amino acid sequences of KR-12 and its analogs generated in this study are summarized in Table 1. To design each peptide sequence, we used the  $\alpha$ -helical wheel projections of peptides shown in Figure 1. As shown in its  $\alpha$ -helical wheel projection, the starting molecule, KR-12, adopted an amphipathic  $\alpha$ -helical structure by converging the hydrophobic residues to one side and the hydrophilic residues to the other side of the helical axis (Figure 1). Several studies suggested that AMPs containing Trp display more potent antimicrobial activity than those with either Phe or Tyr. The bulkier Trp side chain may ensure a more efficient interaction with membrane surfaces, allowing the peptides to partition in the bilayer interface [18–20]. Some reports showed that the best position for Trp-substitution in  $\alpha$ -helical peptide to design novel  $\alpha$ -helical AMPs is the amphipathic interface between the end of the hydrophilic side and the start of the hydrophobic side of its  $\alpha$ -helical wheel projection [21–23]. For this reason, KR-12-a1 was designed by replacing Phe<sup>10</sup> (the amphipathic interface position in  $\alpha$ -helical wheel projection of KR-12) with Trp. KR-12-a2 and KR-12-a3 are obtained by substituting Asp<sup>9</sup> or/and Gln<sup>5</sup> with Lys to get increase in positive charge. KR-12-a4, KR-12-a5 and KR-12-a6 from KR-12-a3 were designed to increase hydrophobic angle by substituting more Leu residues. KR-12-a7 and KR-12-a8 from KR-12-a3 were generated to increase hydrophilic angle by

substituting more Lys residues. The observed and calculated molecular weights of synthesized peptides were in agreement (Table 1). The physiochemical properties of KR-12 and its analogs were shown in Table 1.

### 3.2 Secondary Structure Studies using CD Spectroscopy

The CD spectra for all the peptides in 10mM sodium phosphate buffer (pH 7.2) displayed a negative band at approximately 200 nm, indicating that the structure is random (Figure 2-a). All the peptides showed characteristic  $\alpha$ -helical CD spectra with two dichroic minimal values at 208 and 222 nm and a positive band near 192 nm (Figure 2-b). Among these peptides, KR-12-a8 had showed least  $\alpha$ -helical structure.

### 3.3 Antimicrobial and Hemolytic Activities

The antimicrobial activity of KR-12 and its analogs was tested against three Gram-positive bacteria (*B. subtilis*, *S. epidermidis* and *S.aureus*) and three Gram-negative bacteria (*E. coli*, *P. aeruginosa* and *S. typhimurium*) (Table 2). Compared to the activity of parent peptide LL-37, all peptides showed equal or higher activity (Table 2). Except for KR-12-a6, KR-12 and most of its analogs were likewise similarly effective when assessed using the geometric mean (GM) (2.5–4.2  $\mu$ M) of the MIC values from all selected microbial strains, as an overall measure of the antimicrobial activity of the peptides (Table 3). In particular, KR-12-a6 showed the weakest antimicrobial activity against *E. coli* and *P. aeruginosa*. For a quantitative measure of the hemolytic activity of the peptides, we introduced the hemolytic concentration (HC<sub>50</sub>) defined as the lowest peptide concentration that produces 50% hemolysis against human red blood cells (Figure 3 and Table 3). Hemolytic activities of the peptides were highly significantly

lower than that of LL-37. Except for KR-12-a5 and KR-12-a6, most of KR-12 analogs did not show 50% hemolysis even at high concentration as 800  $\mu\text{M}$  (Figure 3 and Table 3). KR-12-a5 and KR-12-a6 had  $\text{HC}_{50}$  values 96  $\mu\text{M}$  and 22  $\mu\text{M}$ , respectively.

### 3.4 Cell Specificity (Therapeutic Index)

The therapeutic potential of antimicrobial agents lies in the cell specificity for bacteria over erythrocytes. Cell specificity is a measure of peptide's capability to differentiate any pathogen against host cells. It is one of the most difficult challenges in the development of antimicrobial agents, especially if the target of action is the cytoplasmic membrane. Cell specificity of the peptides is expressed as the therapeutic index (TI) =  $\text{HC}_{50}/\text{GM}$ , where  $\text{HC}_{50}$  is peptide concentration needed to reach 50% lysis of human red blood cells, while GM is expressed as the geometric mean of MICs against six bacterial cells. The TI is a widely accepted parameter to represent the specificity of antimicrobial agents between bacterial and mammalian cells [24–27]. Larger values of TI indicate greater cell specificity. The TI values of KR-12 and its designed analogs are shown in Table 3. Except for KR-12-a5, KR-12-a6, KR-12, other KR-12 analogs showed an increase in TI by more than 16–24-fold, relative to parental LL-37. KR-12-a5 displayed almost same TI value when compared to LL-37.

### 3.5 Anti-MRSA Activity

Methicillin-resistant *Staphylococcus aureus* (MRSA) strains, which have become resistant to most antibiotics, are most often found associated with institutions such as hospitals, but they are also becoming increasingly prevalent in community-acquired infections[28, 29]. KR-12-a2, KR-12-a3 and KR-12-a4 having cell specificity and



antiendotoxic activity exhibited good anti-MRSA activity. These peptides displayed the MIC value of 4  $\mu\text{M}$  against three MRSA strains.

### **3.6 Cytotoxicity toward RAW264.7 Cells**

In addition to hemolytic activity, RAW264.7 macrophage cells were used to evaluate cytotoxicity against mammalian cells (Figure 4). Similar to hemolytic activity of the peptides, the cytotoxicity towards RAW264.7 cells also increased with hydrophobicity. As shown in Fig. 4, KR-12-a4, KR-12-a5 and KR-12-a6 were non-toxic to RAW264.7 cells until 12.5 $\mu\text{M}$ , respectively. In contrast, other KR-12 analogs did not show a significant cytotoxicity even at 100  $\mu\text{M}$ . Therefore, antiendotoxic activity of the peptides using RAW264.7 macrophage cells was conducted at concentration less than 12.5 $\mu\text{M}$ .

### **3.7 Antiendotoxic Activity (Anti-LPS activity)**

Several natural, analogs and *de novo* designed peptides are reported to have LPS neutralization activity [2, 30–34]. The suggested mechanism for LPS neutralization is that the peptides binds to the LPS and change the structure from cubic lamellar into multilamellar form and thereby preventing the binding of LPS to host proteins involved in inflammation pathways [2, 32]. LL-37 was shown to have the ability to displace the bounded LPS from macrophages [2], which is highly desirable for a potential drug. Thus, we have investigated the ability of KR-12 and its analogs to neutralize the LPS mediated cytokine release. TNF- $\alpha$  is one of the first proinflammatory cytokines secreted by LPS-stimulated immune cells [35]. To evaluate the antiendotoxic activity of KR and its analogs, LPS-induced TNF- $\alpha$  production was evaluated in macrophage cell, RAW

264.7, in the absence and presence of these peptides by ELISA experiment (Figure 5). We observed that KR-12-a2, KR-12-a3, KR-12-a4, KR-12-a5 and KR-12-a6 efficiently inhibited the production of TNF- $\alpha$  from LPS-stimulated RAW 264.7 cells at 10 $\mu$ M, whereas other peptides (KR-12, KR-12-a1, KR-12-a7 and KR-12-a 8) were less active in inhibiting the production of TNF- $\alpha$  from these cells (Figure 5 and Table 3). Among KR-12 analogs, both KR-12-a5 and KR-12-a6 with higher hydrophobicity showed greater inhibiting activity on LPS-induced TNF- $\alpha$  production.

LPS-neutralizing activity such as the inhibition of TNF- $\alpha$  production of AMPs lies in the binding LPS and then disintegration of the LPS core region takes place which is primarily constituted of lipid A. To investigate correlation between LPS-neutralizing activity and LPS binding activity of KR-12 and its analogs, the binding activity of the peptides to LPS was conducted by chromogenic *limulus amoebocyte* lysate (LAL) assay. Binding of the peptides to LPS was determined by measuring their efficacy to inhibit the LPS-induced activation of LAL enzyme. In the LAL assay, KR-12-a5 and KR-12-a6 displayed the highest LPS-binding activity (Figure 6). The ability of the peptides to bind to LPS was in accordance with their LPS-neutralizing activity. However, KR-12-a2 and KR-12-a3 showed potent LPS-neutralizing activity, but their direct LPS binding affinity is considerably lower than KR-12-a5 and KR-12-a6. This can be arising from another factor that cathelicidin-derived AMPs are able to bind directly with proteins of LPS signaling complex and thereby blocking the binding of LPS with its downstream proteins [4, 36]. Further studies are required to explore these possibilities.

There was no linear correlation between the positive charge and LPS binding or LPS-neutralizing activity. KR-12 and KR-12-a1 having a net positive charge of +5 did not show any LPS-neutralizing activity and LPS-binding affinity. However, KR-12-a2

and KR-12-a3 with a net positive charge of +7 and +8, respectively, but less hydrophobic compared to KR-12 and KR-12-a1. These peptides displayed higher LPS-neutralizing activity than KR-12 and KR-12-a1. KR-12-a4 with relatively higher net positive charge (+7) and hydrophobicity had lower LPS-neutralizing activity than KR-12-a2 and KR-12-a3. KR-12-a5 and KR-12-a6 bearing positive charge of +5 or +6 and highest hydrophobicity caused much higher LPS-neutralizing activity and LPS-binding activity as compared to KR-12-a7 and KR-12-a8 having positive charge of +9 or +10. These results suggested that a delicate balance between hydrophobicity and charge of the peptides is required for optimal activity for LPS neutralization. Rosenfeld *et.al.* reported that an increase in ratio between hydrophobicity and charge of peptides will increase both antimicrobial and LPS neutralization effect [37].

Even though KR-12-a5 and KR-12-a6 showed higher LPS binding activity, their corresponding MIC values are slightly higher than that of other peptides against Gram-negative bacteria. This may be due to the lower efficiency of these peptides on other factors that determines the inhibition of bacterial growth.

## 4. Conclusion

In the present study, we optimized novel short KR-12 analogs (KR-12-a2, KR-12-a3 and KR-12-a4) possessing both antimicrobial anti-inflammatory activities without mammalian cytotoxicity. Also, these peptides exhibited anti-MRSA activity. All of these properties make KR-12 analogs good candidates for the development of antimicrobial and anti-inflammatory agents.

**Table 1.** Amino acid sequences and physicochemical properties of KR-12 and its analogs used for comparison

Peptides	Amino acid sequences	Molecular mass		Net charge	H <sup>b</sup>	[θ] <sup>c</sup> ; f <sub>α</sub> <sup>d</sup>
		Calculated	Observed <sup>a</sup>			
KR-12	KRIVQRIKDFLR-NH <sub>2</sub>	1570.9	1570.8	+5	-0.47	-22.72; 0.64
KR-12-a1	KRIVQRIKDWLR-NH <sub>2</sub>	1609.9	1610.1	+5	-0.49	-18.29; 0.50
KR-12-a2	KRIVQRIKKWLR-NH <sub>2</sub>	1623.1	1622.7	+7	-0.53	-18.27; 0.50
KR-12-a3	KRIVKRIKKWLR-NH <sub>2</sub>	1623.1	1623.7	+8	-0.56	-14.66; 0.39
KR-12-a4	KRIVKLIKKWLR-NH <sub>2</sub>	1580.1	1580.9	+7	-0.37	-19.95; 0.55
KR-12-a5	KRIVKLILKWLR-NH <sub>2</sub>	1565.1	1565.2	+6	-0.23	-20.62; 0.57
KR-12-a6	LRIVKLILKWLR-NH <sub>2</sub>	1550.0	1551.1	+5	-0.10	-10.39; 0.26
KR-12-a7	KRIRKRIKKWLR-NH <sub>2</sub>	1680.2	1680.5	+9	-0.75	-16.46; 0.48
KR-12-a8	KRIRKRIKKWKR-NH <sub>2</sub>	1695.2	1695.3	+10	-0.89	-10.53; 0.27

<sup>a</sup>Molecular mass were determined using MALDI-TOF-MS. Bold letters are substituted amino acids.

<sup>b</sup>H = mean hydrophobicity, as calculated using the HydroMCalc applet (<http://www.bbcm.univ.trieste.it/~tossi/HydroCalc/HydroMCalc.html>), not considering the amidated C-termini.

<sup>c</sup>Units of 10<sup>3</sup> × (deg · cm<sup>2</sup> · d mol<sup>-1</sup>)

<sup>d</sup>The formula  $f_{\alpha} = (\theta - \theta_{RC}) / (\theta_H - \theta_{RC})$  was used to estimate the fractional helical content  $f_{\alpha}$  of peptides in a helical conformation, where  $\theta$  is observed ellipticity and  $\theta_{RC}$  and  $\theta_H$  are the limiting values for a completely random coil and a completely helical conformation, respectively. Here, we use the following values, both at 222 nm:  $\theta_{RC} = -1.5 \times 10^3 \text{ deg} \cdot \text{cm}^{-2} \cdot \text{d mol}^{-1}$  and  $\theta_H = -33.4 \times 10^3 \text{ deg} \cdot \text{cm}^{-2} \cdot \text{d mol}^{-1}$ .

## 2. Antimicrobial activity of KR-12 and its analogs

Peptides	MIC <sup>a</sup> (μM)					
	Gram-negative bacteria			Gram-positive bacteria		
	<i>E. coli</i>	<i>P. aeruginosa</i>	<i>S. typhimurium</i>	<i>B. subtilis</i>	<i>S. epidermidis</i>	<i>S. aureus</i>
KR-12	2	4	2	8	1	4
KR-12-a1	2	8	4	4	1	2
KR-12-a2	2	8	1	8	1	2
KR-12-a3	2	8	2	2	1	2
KR-12-a4	2	4	1	8	1	2
KR-12-a5	4	8	4	4	1	4
KR-12-a6	16	16	4	8	2	4
KR-12-a7	2	4	2	2	1	4
KR-12-a8	2	2	2	4	2	4
LL-37 <sup>b</sup>	8	8	4	8	8	4

<sup>a</sup>MIC (minimal inhibitory concentration), the lowest peptide concentration for no microbial growth, was determined from three independent experiments in triplicate.

<sup>b</sup>The MIC values of LL-37 were derived from Reference 21.

**Table 3.** Cell specificity (therapeutic index) and antiendotoxic activity of KR-12 and its analogs

Peptides	GM ( $\mu\text{M}$ ) <sup>a</sup>	HC <sub>50</sub> ( $\mu\text{M}$ ) <sup>b</sup>	TI <sup>c</sup> (HC <sub>50</sub> /GM)	Fold <sup>d</sup>	% TNF- $\alpha$ Inhibition <sup>f</sup>
KR-12	3.5	> 800	457	17.6	3.8
KR-12-a1	3.5	> 800	457	17.6	3.4
KR-12-a2	3.7	> 800	432	16.6	58.6
KR-12-a3	2.8	> 800	571	22.0	74.2
KR-12-a4	3.0	> 800	533	20.5	53.2
KR-12-a5	4.2	96	23	0.9	80.7
KR-12-a6	8.3	22	3	0.1	87.7
KR-12-a7	2.5	> 800	640	24.6	3.1
KR-12-a8	2.7	> 800	593	22.8	1.3
LL-37	6.7	175	26	1	93.4

<sup>a</sup> GM denotes the geometric mean of MIC values from all six bacterial strains.

<sup>b</sup> HC<sub>50</sub> is peptide concentration that produces 50% hemolysis of human red blood cells.

<sup>c</sup> Therapeutic index (TI) is the ratio of the HC<sub>50</sub> value ( $\mu\text{M}$ ) over the GM ( $\mu\text{M}$ ).

When 50% hemolysis was not observed at 800 $\mu\text{M}$ , a value of 1600 $\mu\text{M}$  was used for calculation of the HC<sub>50</sub> value.

<sup>d</sup> The fold improvement in therapeutic index compared with that of LL-37.

<sup>f</sup> The percent inhibition of TNF- $\alpha$  production at 10  $\mu\text{M}$ .

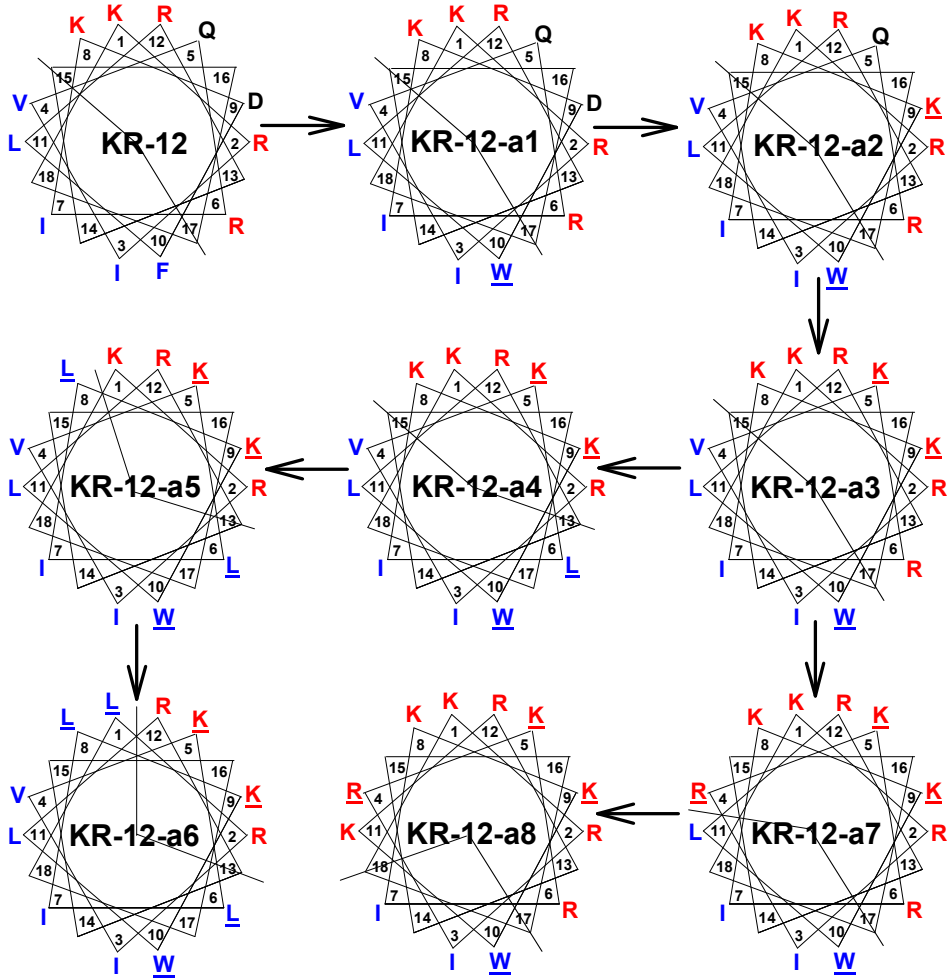


**Figure 1.** Helical wheel diagrams for KR-12 and its analogs designed in this study. The peptide name is presented in the middle of each diagram. The order of design is depicted by the flow of the arrows. The underline indicates substituted-amino acids. The positive charged amino acids and hydrophobic amino acids were represented as the red and blue colors, respectively. The line indicates the interface between the hydrophobic face and the negatively charged face. Unstructured ends of these peptides can slightly change the exact helical wheel representation, and hydrophobic/hydrophilic amino acid distribution.



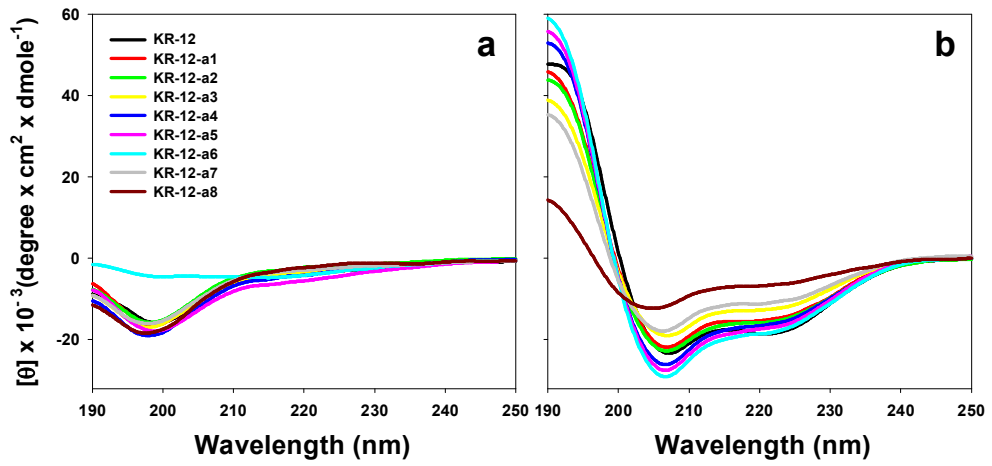


**Figure 2.** Circular dichroism (CD) spectra of the peptides in 10 mM sodium phosphate buffer, pH 7.2 (a) or 0.1% LPS (b)

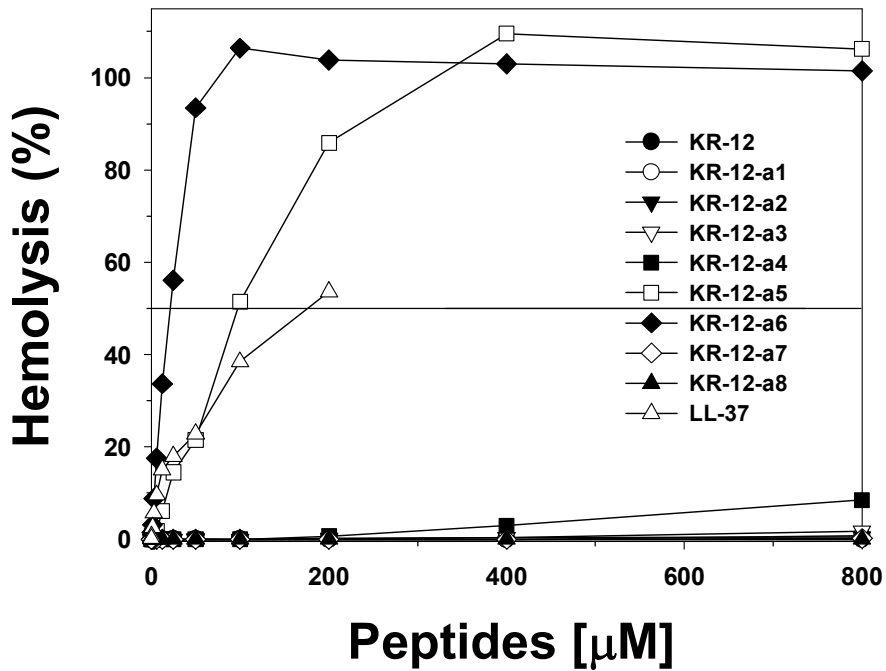


**Figure 3.** Concentration–response curves of percent hemolysis of KR-12 and its analogs against human red blood cells.  $HC_{50}$  is minimal peptide concentration that produces 50% hemolysis of human red blood cells, indicated by middle line parallel to peptide concentration axis.

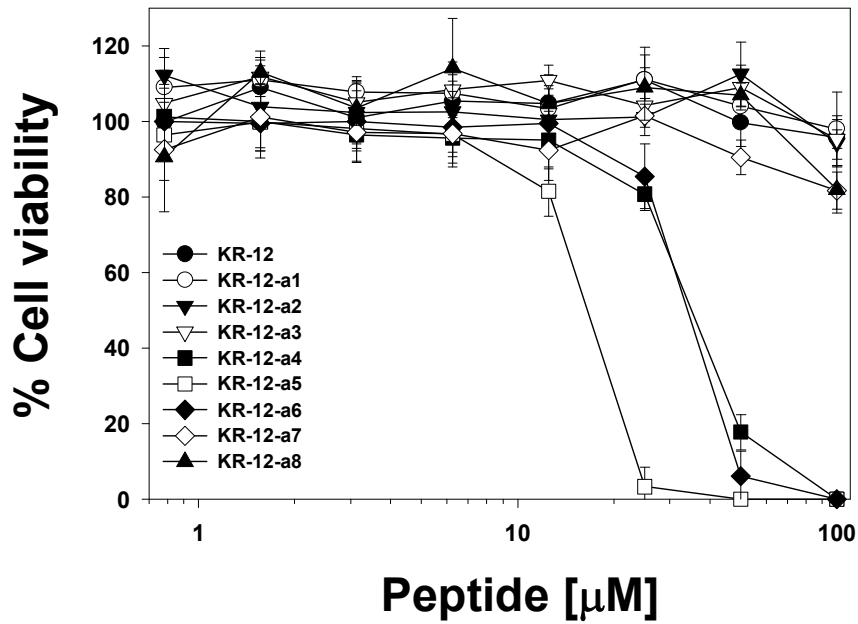


**Figure 4.** Cytotoxicity of KR-12 and its analogs against macrophage-derived RAW264.7 cells.

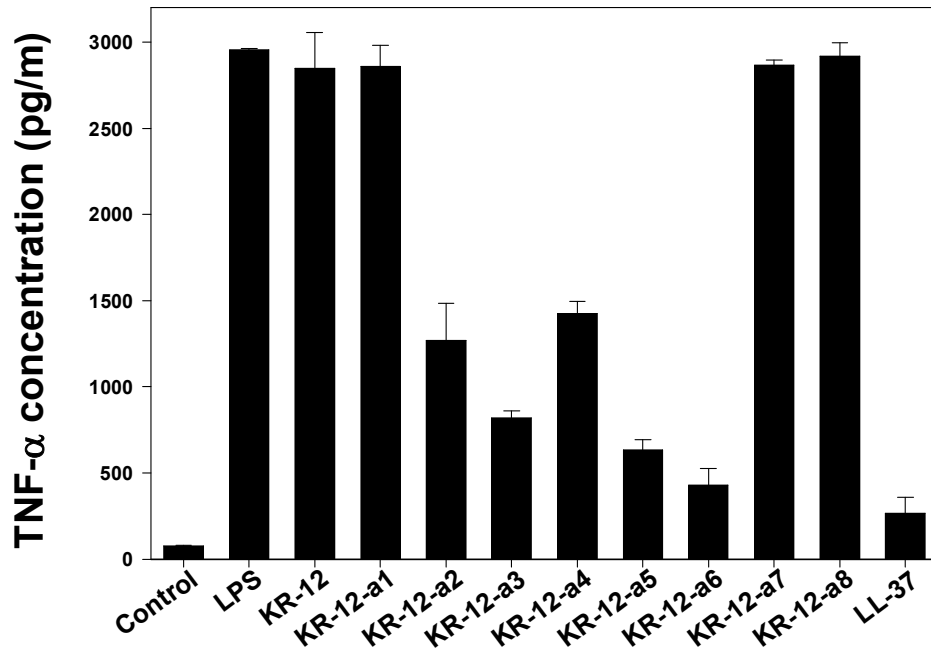


**Figure 5.** Inhibitory effects of KR-12 and its analogs on LPS-stimulated TNF- $\alpha$  production in RAW264.7 cells.

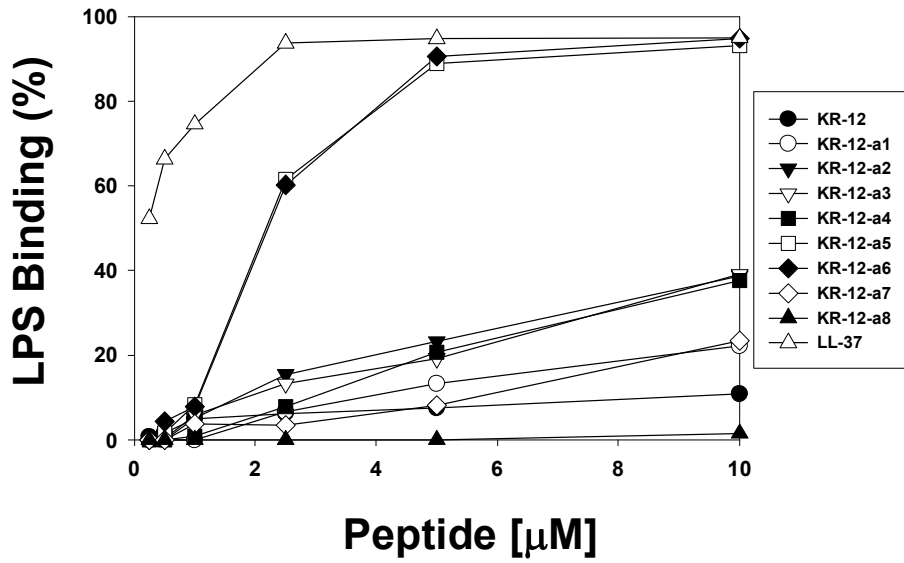


**Figure 6.** Ability of the peptides to bind with LPS was evaluated by Limulus Amebocyte Lysate (LAL) Kinetic-QCL™ according to manufacturer's instructions.

## 5. References

- [1] C.R.H. Raetz, C. Whitfield, Lipopolysaccharide endotoxins., *Annu. Rev. Biochem.* 71 (2002) 635–700. doi:10.1146/annurev.biochem.71.110601.135414.
- [2] Y. Rosenfeld, N. Papo, Y. Shai, Endotoxin (lipopolysaccharide) neutralization by innate immunity host-defense peptides. Peptide properties and plausible modes of action., *J. Biol. Chem.* 281 (2006) 1636–43. doi:10.1074/jbc.M504327200.
- [3] J.C. Chow, D.W. Young, D.T. Golenbock, W.J. Christ, F. Gusovsky, Toll-like Receptor-4 Mediates Lipopolysaccharide-induced Signal Transduction, *J. Biol. Chem.* 274 (1999) 10689–10692. doi:10.1074/jbc.274.16.10689.
- [4] Q. Jiang, S. Akashi, K. Miyake, H.R. Petty, Cutting Edge: Lipopolysaccharide Induces Physical Proximity between CD14 and Toll-Like Receptor 4 (TLR4) Prior to Nuclear Translocation of NF- B, *J. Immunol.* 165 (2000) 3541–3544. doi:10.4049/jimmunol.165.7.3541.
- [5] Y. Rosenfeld, Y. Shai, Lipopolysaccharide (Endotoxin)-host defense antibacterial peptides interactions: role in bacterial resistance and prevention of sepsis., *Biochim. Biophys. Acta.* 1758 (2006) 1513–22. doi:10.1016/j.bbame.2006.05.017.
- [6] J. Cohen, The immunopathogenesis of sepsis, 420 (2002) 885–891.
- [7] H.G. Boman, Peptide antibiotics and their role in innate immunity., *Annu. Rev. Immunol.* 13 (1995) 61–92. doi:10.1146/annurev.iy.13.040195.000425.
- [8] M. Zasloff, Antimicrobial peptides of multicellular organisms., *Nature.* 415 (2002) 389–95. doi:10.1038/415389a
- [9] J. Johansson, Conformation-dependent Antibacterial Activity of the Naturally Occurring Human Peptide LL-37, *J. Biol. Chem.* 273 (1998) 3718–3724. doi:10.1074/jbc.273.6.3718.
- [10] J.W. Larrick, M. Hirata, R.F. Balint, J. Lee, J. Zhong, S.C. Wright, Human CAP18: a novel antimicrobial lipopolysaccharide-binding protein., *Infect. Immun.* 63 (1995) 1291–7.
- [11] C.D. Ciornei, T. Sigurdardóttir, A. Schmidtchen, M. Bodelsson, Antimicrobial and chemoattractant activity, lipopolysaccharide neutralization, cytotoxicity, and inhibition by serum of analogs of human cathelicidin LL-37., *Antimicrob. Agents Chemother.* 49 (2005) 2845–50. doi:10.1128/AAC.49.7.2845-2850.2005.

- [12] T. Sawa, K. Kurahashi, M. Ohara, M.A. Gropper, V. Doshi, J.W. Larrick, et al., Evaluation of Antimicrobial and Lipopolysaccharide-Neutralizing Effects of a Synthetic CAP18 Fragment against *Pseudomonas aeruginosa* in a Mouse Model, *Antimicrob. Agents Chemother.* 42 (1998) 3269–3275.
- [13] I. Nagaoka, S. Hirota, F. Niyonsaba, M. Hirata, Y. Adachi, H. Tamura, et al., Cathelicidin Family of Antibacterial Peptides CAP18 and CAP11 Inhibit the Expression of TNF- $\alpha$  by Blocking the Binding of LPS to CD14<sup>+</sup> Cells, *J. Immunol.* 167 (2001) 3329–3338. doi:10.4049/jimmunol.167.6.3329.
- [14] I. Nagaoka, S. Hirota, F. Niyonsaba, M. Hirata, Y. Adachi, H. Tamura, et al., Augmentation of the Lipopolysaccharide-Neutralizing Activities of Human Cathelicidin CAP18/LL-37-Derived Antimicrobial Peptides by Replacement with Hydrophobic and Cationic Amino Acid Residues, *Clin. Vaccine Immunol.* 9 (2002) 972–982. doi:10.1128/CDLI.9.5.972-982.2002.
- [15] R.M. Dawson, J. McAllister, C.-Q. Liu, Characterisation and evaluation of synthetic antimicrobial peptides against *Bacillus globigii*, *Bacillus anthracis* and *Burkholderia thailandensis*, *Int. J. Antimicrob. Agents.* 36 (2010) 359–63. doi:10.1016/j.ijantimicag.2010.06.038.
- [16] G. Wang, Structures of human host defense cathelicidin LL-37 and its smallest antimicrobial peptide KR-12 in lipid micelles., *J. Biol. Chem.* 283 (2008) 32637–43. doi:10.1074/jbc.M805533200.
- [17] A.S. Ladokhin, S.H. White, Folding of amphipathic alpha-helices on membranes: energetics of helix formation by melittin., *J. Mol. Biol.* 285 (1999) 1363–9. doi:10.1006/jmbi.1998.2346.
- [18] W. Hu, K.C. Lee, T.A. Cross, Tryptophans in membrane proteins: Indole ring orientations and functional implications in the gramicidin channel, *Biochemistry.* 32 (1993) 7035–7047. doi:10.1021/bi00078a032.
- [19] D. Oh, S.Y. Shin, S. Lee, J.H. Kang, S.D. Kim, P.D. Ryu, et al., Role of the Hinge Region and the Tryptophan Residue in the Synthetic Antimicrobial Peptides, Cecropin A(1–8)–Magainin 2(1–12) and Its Analogues, on Their Antibiotic Activities and Structures †, ‡, *Biochemistry.* 39 (2000) 11855–11864. doi:10.1021/bi000453g.
- [20] K. Park, D. Oh, S.Y. Shin, K.-S. Hahm, Y. Kim, Structural studies of porcine myeloid antibacterial peptide PMAP-23 and its analogues in DPC micelles by NMR spectroscopy., *Biochem. Biophys. Res. Commun.* 290 (2002) 204–12. doi:10.1006/bbrc.2001.6173.
- [21] Y.H. Nan, J.-K. Bang, B. Jacob, I.-S. Park, S.Y. Shin, Prokaryotic selectivity and LPS-neutralizing activity of short antimicrobial peptides designed from the

- human antimicrobial peptide LL-37., *Peptides*. 35 (2012) 239–47. doi:10.1016/j.peptides.2012.04.004.
- [22] S.-J. Kim, J.-S. Kim, Y.-S. Lee, D.-W. Sim, S.-H. Lee, Y.-Y. Bahk, et al., Structural characterization of de novo designed L5K5W model peptide isomers with potent antimicrobial and varied hemolytic activities. *Molecules*. 18 (2013) 859–76. doi:10.3390/molecules18010859.
- [23] S.-J. Kang, H.-S. Won, W.-S. Choi, B.-J. Lee, De novo generation of antimicrobial LK peptides with a single tryptophan at the critical amphipathic interface. *J. Pept. Sci.* 15 (2009) 583–8. doi:10.1002/psc.1149.
- [24] Y. Chen, C.T. Mant, S.W. Farmer, R.E.W. Hancock, M.L. Vasil, R.S. Hodges, Rational design of alpha-helical antimicrobial peptides with enhanced activities and specificity/therapeutic index., *J. Biol. Chem.* 280 (2005) 12316–29. doi:10.1074/jbc.M413406200.
- [25] M.A. Fázio, L. Jouvensal, F. Vovelle, P. Bulet, M.T.M. Miranda, S. Daffre, et al., Biological and structural characterization of new linear gomesin analogues with improved therapeutic indices. *Biopolymers*. 88 (2007) 386–400. doi:10.1002/bip.20660.
- [26] J.-K. Kim, S.-A. Lee, S. Shin, J.-Y. Lee, K.-W. Jeong, Y.H. Nan, et al., Structural flexibility and the positive charges are the key factors in bacterial cell selectivity and membrane penetration of peptoid-substituted analog of Piscidin 1., *Biochim. Biophys. Acta*. 1798 (2010) 1913–25. doi:10.1016/j.bbamem.2010.06.026.
- [27] P. Wang, Y.H. Nan, S.-T. Yang, S.W. Kang, Y. Kim, I.-S. Park, et al., Cell selectivity and anti-inflammatory activity of a Leu/Lys-rich alpha-helical model antimicrobial peptide and its diastereomeric peptides., *Peptides*. 31 (2010) 1251–61. doi:10.1016/j.peptides.2010.03.032.
- [28] L. Kardas-Sloma, P.Y. Boëlle, L. Opatowski, C. Brun-Buisson, D. Guillemot, L. Temime, Impact of antibiotic exposure patterns on selection of community-associated methicillin-resistant *Staphylococcus aureus* in hospital settings., *Antimicrob. Agents Chemother.* 55 (2011) 4888–95. doi:10.1128/AAC.01626-10.
- [29] M.Z. David, D. Glikman, S.E. Crawford, J. Peng, K.J. King, M.A. Hostetler, et al., What is community-associated methicillin-resistant *Staphylococcus aureus*?, *J. Infect. Dis.* 197 (2008) 1235–43. doi:10.1086/533502.
- [30] M. Gough, R.E. Hancock, N.M. Kelly, Antiendotoxin activity of cationic peptide antimicrobial agents, *Infect. Immun.* 64 (1996) 4922–7.
- [31] Y. Kaconis, I. Kowalski, J. Howe, A. Brauser, W. Richter, I. Razquin-Olazarán,



- et al., Biophysical mechanisms of endotoxin neutralization by cationic amphiphilic peptides., *Biophys. J.* 100 (2011) 2652–61. doi:10.1016/j.bpj.2011.04.041.
- [32] S. Bhattacharjya, De novo designed lipopolysaccharide binding peptides: structure based development of antiendotoxic and antimicrobial drugs. *Curr. Med. Chem.* 17 (2010) 3080–93.
- [33] G.H. Zhang, D.M. Mann, C.M. Tsai, Neutralization of endotoxin in vitro and in vivo by a human lactoferrin-derived peptide. *Infect. Immun.* 67 (1999) 1353–8.
- [34] M.J. Nell, G.S. Tjabringa, A.R. Wafelman, R. Verrijck, P.S. Hiemstra, J.W. Drijfhout, et al., Development of novel LL-37 derived antimicrobial peptides with LPS and LTA neutralizing and antimicrobial activities for therapeutic application., *Peptides.* 27 (2006) 649–60. doi:10.1016/j.peptides.2005.09.016.
- [35] F.X. Zhang, C.J. Kirschning, R. Mancinelli, X.-P. Xu, Y. Jin, E. Faure, et al., Bacterial Lipopolysaccharide Activates Nuclear Factor- B through Interleukin-1 Signaling Mediators in Cultured Human Dermal Endothelial Cells and Mononuclear Phagocytes, *J. Biol. Chem.* 274 (1999) 7611–7614. doi:10.1074/jbc.274.12.7611.
- [36] N. Mookherjee, H.L. Wilson, S. Doria, Y. Popowych, R. Falsafi, J.J. Yu, et al., Bovine and human cathelicidin cationic host defense peptides similarly suppress transcriptional responses to bacterial lipopolysaccharide. *J. Leukoc. Biol.* 80 (2006) 1563–74. doi:10.1189/jlb.0106048.
- [37] Y. Rosenfeld, N. Lev, Y. Shai, Effect of the hydrophobicity to net positive charge ratio on antibacterial and anti-endotoxin activities of structurally similar antimicrobial peptides., *Biochemistry.* 49 (2010) 853–61. doi:10.1021/bi900724x.

## **PART II**

**Bacterial killing mechanism of sheep myeloid antimicrobial peptide-18 (SMAP-18) and its Trp-substituted analog with improved cell selectivity and reduced mammalian cell toxicity**

## 1. Introduction

The cathelicidins are a large family of structurally diverse antimicrobial peptides (AMPs) found in mammalian species including humans [1,2]. All members of the cathelicidin family contain an N-terminal cathelin domain and a C-terminal domain of varied structure that displays antimicrobial activity after being freed by proteolytic processing of the holoprotein [3,4]. Among these, sheep myeloid antimicrobial peptide-29 (SMAP-29) is a 28 residue  $\alpha$ -helical cathelicidin-derived AMP with an amidated C-terminus [5]. Another form of SMAP-29 also exist which is having 29-residue and non-amidated carboxyl terminal [6]. In this study, 28-residue amidated peptide will be referred as SMAP-29. SMAP-29 display potent and broad-spectrum antimicrobial activity against gram-negative and gram-positive bacteria and fungi [5,6]. However, it is also highly cytotoxic both to human red blood cells (hRBCs) and human embryonic kidney (HEK) cells[7]. The cytotoxicity against human normal cells of SMAP-29 is a major barrier for developing it into a novel therapeutic antimicrobial agent. The antimicrobial activity of SMAP-29 has been attributed to the N-terminal amphipathic  $\alpha$ -helix region (residues 1–18), and the hemolytic activity to the hydrophobic C-terminal region (residues 19–29) [8]. A number of variants of SMAP-29 have been prepared in an attempt to improve the cell selectivity for pathogenic microorganisms over mammalian cells [8,9].

In this study, therefore, to develop short AMPs with improved cell selectivity and reduced mammalian cell toxicity compared to SMAP-29 and explore the possible mechanisms responsible for their antimicrobial action, we synthesized SMAP-29 (1-18)

amide with amidated C-termini (hereafter called SMAP-18) corresponding to N-terminal amphipathic  $\alpha$ -helical domain. Previous study had shown that the N-terminal region is responsible for the antimicrobial activity of SMAP-29 [8]. SMAP-29 has two  $\alpha$ -helical regions connected by a hinge region consisting of Gly and Pro. The carboxyl terminal region is more hydrophobic and may be responsible for higher hemolytic activity of SMAP-29. Other studies also showed that analogs of N-terminal region of SMAP-29 showed potent antimicrobial activity with lower hemolytic activity [9].

Several studies suggested that AMPs containing Trp display more potent antimicrobial activity than those with either Phe or Tyr. The bulkier Trp side chain may ensure a more efficient interaction with membrane, allowing the peptides to partition in the bilayer interface [10–12]

. For this reason, SMAP-18 analog (SMAP-18-W) was designed by replacing Leu, Leu, Ile and Val residues at positions 3, 6, 10 and 14 of SAMP-18 with Trp. The cell selectivity of the peptides was investigated by examining their antimicrobial activity against Gram-positive and Gram-negative bacterial strains and their hemolytic activity against human red blood cells. The cytotoxicity of these peptides against three different types of mammalian cells (mouse macrophage RAW 264.7, mouse fibroblastic NIH-3T3 cells and human cervical carcinoma HeLa cells) was evaluated. Furthermore, to gain insight the mechanism of bacterial killing action of the peptides, we performed fluorescent dye leakage assay, membrane depolarization assay, time-killing kinetics, N-phenyl-1-naphthylamine (NPN) assay (outer membrane permeability), o-nitrophenyl- $\beta$ -galactoside (ONPG) hydrolysis assay (inner membrane permeability) and confocal laser scanning microscopy.

## 2. Materials and methods

### 2.1 Materials

Rink amide 4-methylbenzhydrylamine (MBHA) resin and 9-fluorenylmethoxycarbonyl (Fmoc) amino acids were obtained from Calbiochem-Novabiochem (La Jolla, CA, USA). Other reagents used for peptide synthesis included TFA (Sigma, St. Louis, MO, USA), piperidine (Merck, Darmstadt, Germany), DCC (Fluka, Buchs, Switzerland), HOBT (Aldrich) and DMF (peptide synthesis grade; Biolab). DiSC<sub>3-5</sub> was obtained from Molecular Probes (Eugene, OR, USA). EYPE, EYPG, EYPC, cholesterol, gramicidin D, calcein and NPN, ONPG were supplied by Sigma Chemical Co. (St. Louis, MO, USA). DMEM and FBS were supplied by HyClone (SeouLin, Bioscience, Korea). *Escherichia coli* ML-35, a lactose, permease-deficient strain with constitutive cytoplasmic 3-galactosidase activity (*lacIIacZ<sup>+</sup> lacY*), utilized for inner membrane permeability assays, was obtained from Prof. Jae Il Kim, School of Life Science, Gwangju Institute of Science and Technology (GIST), Gwangju, Republic of Korea. All other reagents were of analytical grade. The buffers were prepared in double glass-distilled water.

### 2.2 Peptide Synthesis

SMAP-29, SMAP-18 and SMAP-18-W shown in Table 1 were synthesized by the standard Fmoc-based solid-phase method on rink amide 4-methylbenzhydrylamine resin (0.54 mmol/g). DCC and HOBT were used as coupling reagents, and tenfold excess Fmoc-amino acids were added during every coupling cycle. After cleavage and deprotection with a mixture of

TFA/water/thioanisole/phenol/ethanedithiol/triisopropylsilane (81.5 : 5 : 5 : 5 : 2.5:1, v/v/v/v/v/v) for 2 h at room temperature, the crude peptide was repeatedly extracted with diethyl ether and purified by RP-HPLC on a preparative Vydac C18 column (20 mm ×250 mm, 300 Å, 15-mm particle size) using an appropriate 0–90% water/acetonitrile gradient in the presence of 0.05% TFA. The final purity of the peptides (>95%) was assessed by RP-HPLC on an analytical Vydac C18 column (4.6 ×250 mm, 300 Å, 5-mm particle size). The molecular mass of synthetic peptides was determined by MALDI-TOF MS (Shimadzu, Kyoto, Japan) (Table 1).

### 2.3 Antimicrobial Assay

The antimicrobial activity of the peptides against three Gram-positive bacterial strains and three gram-negative bacterial strains was examined by using the broth microdilution method in sterile 96-well plates. Aliquots (100 µl) of a bacterial suspension at  $2 \times 10^6$  CFU/ml in 1% peptone were added to 100 µl of the peptide solution (serial 2-fold dilutions in 1% peptone). After incubation for 18–20 h at 37°C, bacterial growth inhibition was determined by measuring the absorbance at 600 nm with a Microplate Autoreader EL 800 (Bio-Tek Instruments, VT). The minimal inhibitory concentration (MIC) was defined as the lowest peptide concentration that causes 100% inhibition of microbial growth. Two types of gram-positive bacteria (*Staphylococcus epidermidis* [KCTC 1917] and *Staphylococcus aureus* [KCTC 1621]) and three types of gram-negative bacteria (*Escherichia coli* [KCTC 1682], *Pseudomonas aeruginosa* [KCTC 1637] and *Salmonella typhimurium* [KCTC 1926]) were procured from the Korean Collection for Type Cultures (KCTC) at the Korea Research Institute of Bioscience and Biotechnology (KRIBB).

#### 2.4. Measurement of Hemolytic Activity

The hemolytic activity of the peptides was measured as the amount of hemoglobin released by the lysis of human erythrocytes [13]. Fresh human red blood cells (hRBCs) were centrifuged, washed three times with PBS (35 mM phosphate buffer, 0.15 M NaCl, pH 7.4), dispensed into 96-well plates as 100  $\mu$ l of 4% (v/v) hRBC in PBS, and 100  $\mu$ l of peptide solution was added to each well. Plates were incubated for 1 h at 37 °C, then centrifuged at 1000  $\times$  g for 5 min. Samples (100  $\mu$ l) of supernatant were transferred to 96-well plates and hemoglobin release was monitored by measuring absorbance at 414 nm. Zero hemolysis was determined in PBS ( $A_{\text{PBS}}$ ) and 100% hemolysis was determined in 0.1% (v/v) Triton X-100 ( $A_{\text{triton}}$ ). The hemolysis percentage hemolysis was calculated as: % hemolysis =  $100 \times [(A_{\text{sample}} - A_{\text{PBS}}) / (A_{\text{triton}} - A_{\text{PBS}})]$

#### 2.5 Mammalian Cell Culture

RAW 264.7, NIH-3T3 and HeLa cells were purchased from the American Type Culture Collection (Manassas, VA) and cultured in DMEM supplemented with 10% fetal bovine serum and antibiotic-antimycotic solution (100 units/ml penicillin, 100  $\mu$ g/ml streptomycin and 25  $\mu$ g/ml amphotericin B) in 5% CO<sub>2</sub> at 37 °C. Cultures were passed every 3 to 5 days, and cells were detached by brief trypsin treatment, and visualized with an inverted microscope.

#### 2.6 Cytotoxicity against Mammalian Cells

Cytotoxicity of peptides against RAW 264.7, NIH-3T3 and HeLa was determined using the MTT proliferation assay as reported previously with minor modifications[14]. The

cells were seeded on 96-well microplates at a density of  $2 \times 10^4$  cells/well in 150  $\mu$ l DMEM containing 10% fetal bovine serum. Plates were incubated for 24 h at 37 °C in 5% CO<sub>2</sub>. Peptide solutions (20  $\mu$ l) (serial 2-fold dilutions in DMEM) were added, and the plates further incubated for 2 days. Wells containing cells without peptides served as controls. Subsequently, 20  $\mu$ l MTT solution (5 mg/ml) was added in each well, and the plates were incubated for a further 4 h at 37 °C. Precipitated MTT formazan was dissolved in 40  $\mu$ l of 20% (w/v) SDS containing 0.01 M HCl for 2h. Absorbance at 570 nm was measured using a microplate ELISA reader (Molecular Devices, Sunnyvale, CA). Cell survival was expressed as a percentage of the ratio of A<sub>570</sub> of cells treated with peptide to that of cells only.

## 2.7. Dye Leakage Assay

Calcein-entrapped LUVs composed of EYPE/EYPG (7:3, w/w) and EYPC/cholesterol (10:1, w/w) were prepared by vortexing the dried lipid in dye buffer solution (70 mM calcein, 10mM Tris, 150 mM NaCl, 0.1 mM EDTA, pH 7.4). The suspension was subjected to 10 frozen-thaw cycles in liquid nitrogen and extruded 21 times through polycarbonate filters (two stacked 100-nm pore size filters) with a LiposoFast extruder (Avestin, Inc. Canada). Untrapped calcein was removed by gel filtration on a Sephadex G-50 column. The concentration of calcein-entrapped LUVs was determined in triplicate by phosphorus analysis (Barlett1959). Calcein leakage from LUVs was monitored at room temperature by measuring fluorescence intensity at an excitation wavelength of 490 nm and emission wavelength of 520 nm on a model RF-5301PC spectrophotometer. Complete dye release was obtained by using 0.1% Triton X-100.



## 2.8 Membrane Depolarization Assay

The cytoplasmic membrane depolarization activity of the peptides was measured using the membrane potential sensitive dye, diSC<sub>3-5</sub> as previously described [15,16]. Briefly, *Staphylococcus aureus* (KCTC 1621) grown at 37°C with agitation to the mid-log phase (OD<sub>600</sub> = 0.4) was harvested by centrifugation. Cells were washed twice with washing buffer (20 mM glucose, 5 mM HEPES, pH 7.4) and resuspended to OD<sub>600</sub> of 0.05 in similar buffer. The cell suspension was incubated with 20 nM diSC<sub>3-5</sub> until stable reduction of fluorescence was achieved, implying incorporation of the dye into the bacterial membrane. Then KCl was added to a final concentration of 0.1 M to equilibrate K<sup>+</sup> levels. Membrane depolarization was monitored by recording changes in the intensity of fluorescence emission of the membrane potential-sensitive dye, diSC<sub>3-5</sub> (excitation λ = 622 nm, emission λ = 670 nm) after peptide addition. The membrane potential was fully dissipated by adding gramicidin D (final concentration of 0.2 nM). The membrane potential dissipating activity of the peptides is calculated as follows:

$$\% \text{ Membrane depolarization} = 100 \times [(F_p - F_0) / (F_g - F_0)]$$

where  $F_0$  denotes the stable fluorescence value after the addition of the diSC<sub>3-5</sub> dye,  $F_p$  denotes the fluorescence value 5 min after peptide addition, and  $F_g$  denotes the fluorescence signal after gramicidin D addition.

## 2.9 NPN Uptake Assay

The ability of peptides to increase outer membrane permeability of gram-negative bacteria was determined by measuring incorporation of the fluorescent dye NPN into the outer membrane of *Escherichia coli* (KCTC 1682) as previously described [17–19]. Briefly, *Escherichia coli* cells were suspended to a final concentration of OD<sub>600</sub> = 0.05

in 5 mM HEPES buffer, pH 7.2, containing 5 mM KCN. NPN was added to 3 ml of cells in a quartz cuvette to give a final concentration of 10  $\mu$ M and the background fluorescence recorded (excitation  $\lambda$  = 350 nm, emission  $\lambda$  = 420 nm). Aliquots of peptide were added to the cuvette and fluorescence recorded as a function of time until there was no further increase in fluorescence. As outer membrane permeability is increased by addition of peptide, NPN incorporated into the membrane causes an increase in fluorescence.

## 2. 10 ONPG Hydrolysis Assay

Inner membrane permeability was determined by measurement in *Escherichiacoli* ML-35 of  $\beta$ -galactosidase activity using the normally impermeable, chromogenic substrate ONPG as substrate [20,21]. *Escherichia coli* ML-35 were washed in 10 mM sodium phosphate (pH 7.4) containing 100 mM NaCl and resuspended in the same buffer at a final concentration of OD<sub>600</sub> = 0.5 containing 1.5 mM ONPG. The hydrolysis of ONPG to o-nitrophenol over time was monitored spectrophotometrically at 405nm following the addition of peptide samples.

## 2.11 Time Killing Kinetics Assay

The time-killing kinetics of the peptides was assessed using *E. coli* (KCTC 1682) and *S. aureus* (KCTC 1621), as described in previous studies[22,23]. The initial density of the cultures was approximately  $1 \times 10^6$  CFU/ml. After 1, 2, 5, 10, 20 or 40 min of exposure to the peptides at 37°C, 50  $\mu$ l aliquots of serial 10-fold dilutions (up to  $10^{-3}$ ) of the cultures were plated onto Luria-Bertani (LB) agar plates to obtain viability counts. Colonies were counted after incubation for 24 h at 37 °C.

## 2.12 Confocal Laser Scanning Microscopy

*Escherichia coli* (KCTC 1682) and *Staphylococcus aureus* (KCTC 1621) cells in mid-logarithmic phase were harvested by centrifugation, washed three times with 10 mM phosphate buffer saline, pH 7.4. Bacteria ( $10^7$  CFU/ml) cells were incubated with FITC-labeled peptides (5  $\mu$ g/ml) at 37 °C for 30 min. After being incubated, the bacterial cells were pelleted down and washed 3 times with 10 mM phosphate buffer saline, pH 7.4 and immobilized on a glass slide. The FITC-labeled peptides were observed with an Olympus FV1000 confocal laser scanning microscope (Japan). Fluorescent images were obtained with a 488 nm band-pass filter for excitation of FITC.

## 3. Results

### 3.1 Antimicrobial and Hemolytic Activities

We examined the antimicrobial activities of the peptides against a representative set of bacterial strains, including three Gram-negative bacteria (*Escherichia coli*, *Pseudomonas aeruginosa* and *Salmonella typhimurium*) and two Gram-positive bacteria (*Staphylococcus epidermidis* and *Staphylococcus aureus*). As shown in Table 2, both SMAP-18 and SMAP-18-W showed a 2- or 4-fold decreased antimicrobial activity when compared to parental SMAP-29. The cytotoxicity of the peptides to mammalian cells was measured by their hemolytic activity toward human red blood cells (hRBCs) (Figure 1). For a quantitative measure of the hemolytic activity of the peptides, we introduced the hemolytic concentration ( $HC_{50}$ ) defined as the lowest peptide concentration that produces 50% hemolysis (Table 2). SMAP-29 displayed relatively high hemolytic activity with  $HC_{50}$  value of  $86\mu\text{M}$ . However, both SMAP-18 amide and SMAP-18-W amide did not cause hemolysis at the highest concentration tested ( $400\mu\text{M}$ ).

### 3.2 Cytotoxicity against Mammalian Cells

To further look into the toxic activity of these peptides against mammalian cells, the viability against three different types of mammalian cells, the murine macrophage RAW 264.7 and fibroblast NIH-3T3 cells and the human cervical carcinoma HeLa cells, was determined in the presence of these peptides. MTT assay was performed to determine the activity of the mitochondrial dehydrogenase, which ultimately suggests the viability of the cells. The cytotoxicity of each peptide was defined by  $IC_{50}$  (the concentration that

causes 50% growth inhibition for each cell lines). SMAP-29 showed relatively strong cytotoxicity ( $IC_{50} = 16.0 \sim 30\mu\text{M}$ ) against all three different cells (Figure 2). In contrast, both SMAP-18 and SMAP-18-W displayed no or less cytotoxicity ( $IC_{50} > 100 \mu\text{M}$ ) against all three different cells even at  $100 \mu\text{M}$  (Figure 2).

### 3.3 Dye Leakage from Model Membranes

To evaluate the ability of the peptides to permeabilize bacterial and mammalian membranes, we measured their ability to induce leakage of the fluorescent dye calcein from negatively charged EYPE/EYPG (7:3, w/w) LUVs (Figure 3-a, b) and zwitterionic EYPC/cholesterol (10: 1, w/w) LUVs (Figure 3-c, d), respectively. SMAP-29 induced a near-complete dye leakage from EYPE/EYPG (7:3, w/w) and EYPC/cholesterol LUVs (10: 1, w/w) at  $0.5 \mu\text{M}$ . SMAP-18 induced 11% and 20% leakage from EYPE/EYPG (7:3, w/w) and EYPC/cholesterol (10: 1, w/w) LUVs even at  $16\mu\text{M}$ , respectively. SMAP-18-W caused 40% dye leakage from both EYPE/EYPG (7:3, w/w) and EYPC/cholesterol (10: 1, w/w) LUVs.

### 3.4 Membrane Depolarization

The membrane potential sensitive dye diSC<sub>3-5</sub> was used to monitor the cytoplasmic membrane depolarization of *Staphylococcus aureus* cells in the presence of peptides. This dye is distributed between the cells and medium, depending on the cytoplasmic membrane potential, and self-quenches when concentrated inside bacterial cells. If the membrane is depolarized, the probe will be released into the medium, causing a measurable increase in fluorescence. SMAP-29 and SMAP-18-W induced a significant membrane depolarization against *Staphylococcus aureus* in a concentration-dependent

manner and depolarized membrane potential of more than 80% at their  $2 \times \text{MIC}$  (Figure 4-a). In contrast, SMAP-18 did not cause any membrane depolarization even at  $4 \times \text{MIC}$  (Figure 4-a). Membrane depolarization was monitored over a period of 550 s for SMAP-29, SMAP-18 and SMAP-18-W (Figure 4-b). SMAP-29 was fast acting, achieving maximum fluorescence at 80 s. The lag time of SMAP-18-W was much longer, leading to maximum fluorescence be achieved after 200 seconds. The ability of SMAP-29 to depolarize bacterial cells was much greater than of SMAP-18-W. SMAP-29 induced 100% membrane depolarization at  $2\mu\text{M}$ . SMAP-18-W caused approximately 80% membrane depolarization at  $8\mu\text{M}$ . In contrast, SMAP-18 did not depolarize the bacterial cytoplasmic membrane even at  $16\mu\text{M}$ .

### **3.5 Evaluation of Outer Membrane Permeability (NPN uptake)**

The ability of the peptides to permeate the outer membrane of *Escherichia coli* was evaluated by the fluorescence-based NPN uptake. NPN is a hydrophobic fluorescent probe that remains quenched in an aqueous environment but fluoresces strongly in a hydrophobic environment. Destabilization of the bacterial outer membrane allows the dye to enter the damaged membrane, where an increase in fluorescence is measured. As observed in LL-37 and melittin, the outer membrane permeabilization of SMAP-29 was detected in a concentration-dependent manner (Figure 5). In contrast, like to buforin-2, SMAP-18 and SMAP-18-W induced relatively little NPN uptake even at  $16\mu\text{M}$  (Figure 5).

### **3.6 Evaluation of Inner Membrane Permeability (ONPG hydrolysis)**

In order to complete membrane permeabilization, peptides translocation to inner

membrane is one of the critical steps. Inner membrane permeabilization was indicated by influx of nonchromogenic substrate ONPG and subsequently cleaved to the yellow product ONP by  $\beta$ -galactosidase in the cytoplasm. As shown in Figure 6, the inner membrane permeabilization of SMAP-29 was detected in a concentration-dependent manner. SMAP-29 induced inner membrane permeation at a high rate, as reflected in the greater slope of ONPG hydrolysis at 0–80 min. In contrast, SMAP-18 and SMAP-18-W did not induce inner membrane permeation even at 16  $\mu$ M. Also, LL-37 and buforin-2 (used as reference peptides) caused weak or less inner membrane permeation even at 16  $\mu$ M.

### 3.7 Time-Kill Kinetics

To study the bactericidal kinetics of the peptides against Gram-negative and -positive bacteria, time killing analyses were carried out using *E. coli*(KCTC 1682) and *S. aureus* (KCTC 1621) at 0.5  $\times$  MIC. As shown in Figure 7, SMAP-29 completely killed both Gram-negative and -positive bacteria in less than 2 minutes. SMAP-18-W was slower than SAMP-29 but killed bacteria faster than SMAP-18. SMAP-18 took longest time among all peptides.

### 3.8 Confocal Laser Scanning Microscopy

To investigate the action site of SMAP-29, SMAP-18 and SMAP-18-W, their FITC-labeled peptides was incubated with log phase *Escherichia coli* and *Staphylococcus aureus* and their localization was visualized by confocal laser-scanning microscopy (Figure 8). Bacterial cells treated for half an hour with FITC-labeled SMAP-18 and buforin-2 at room temperature appeared as green rods with fluorescence spread

throughout the bacterial cell indicating the internalization of FITC-labeled peptide into the cytoplasm of the bacteria. In contrast, the internalization of FITC-labeled peptide into the cytoplasm of the bacteria was not found in SMAP-29 and SMAP-18-W.



## 4. Discussion

The therapeutic potential of AMPs lies in the cell selectivity for bacteria over human erythrocytes. Cell specificity is a measure of peptide's capability to differentiate any pathogen against host cells. It is one of the most difficult challenges in the development of antimicrobial agents, especially if the target of action is cytoplasmic membrane. The cell selectivity of the peptides is defined by the concept of the therapeutic index (TI) as a measure of the relative safety of the drug [24–29]. Larger values of TI indicate greater cell selectivity. The TI of each peptide was calculated as the ratio of the  $HC_{50}$  (the peptide concentration needed to reach 50% lysis of human red blood cells) value to the GM (geometric mean of MICs against five microorganisms) ( $TI = HC_{50}/GM$ ). As shown in Table 2, SMAP-18 and SMAP-18-W showed higher TI than SMAP-29. In addition to hemolytic activity toward human erythrocytes, the cytotoxicity of the peptides against three mammalian cells including NIH-3T3 fibroblasts, HeLa and RAW264.7 cells were evaluated. Unlike SMAP-29, SMAP-18 and SMAP-18-W were not cytotoxic up to 100 $\mu$ M. These results suggest that SMAP-18 and SMAP-18-W are promising candidates for novel therapeutic antimicrobial agents, complementing conventional antibiotic therapies to combat pathogenic microorganisms.

Bacterial killing effect of the majority of AMPs such as LL-37, melittin and SMAP-29 is considered to be due to their action on the lipid matrix of bacterial cell membranes, either by forming pore/ion channels or disrupting the bilayer (*i.e.* membrane-targeting AMPs) [30–32]. These membrane-targeting AMPs were reported to act mainly by causing membrane lysis either by barrel stave, toroidal pore or carpet-

like mechanisms [33–35]. No single mechanism can be defined for all peptides [36]. Furthermore, membrane disruption mechanisms for a given peptide can vary depending on lipid composition or other environmental conditions, for example melittin and aurein were found to act by three different mechanisms depending on the conditions used [36–40]. In contrast, a few AMPs such as buforin 2 and PR-39 were known to penetrate microbial cell membranes without inducing membrane permeabilization and cause bacterial cell death by inhibiting protein, DNA or RNA synthesis (*i.e.* intracellular-targeting AMPs) [41–44].

To examine whether the cytoplasmic membrane of bacterial cells is the ultimate target of SMAP-18 and SMAP-18-W and to determine their membrane selectivity, the abilities of these peptides to cause leakage of a fluorescent dye entrapped within LUVs composed of negatively charged EYPE/EYPG (7:3, w/w) was tested. SMAP-29 showed very strong dye leakage from bacterial-membrane-mimicking lipid vesicles as melittin does. In contrast, SMAP-18 and SMAP-18-W caused a 20% and 40% leakage from calcein-entrapped negatively charged EYPG/EYPE (7:3, w/w) at 16  $\mu\text{M}$ , respectively. Also, SMAP-29 induced very strong dye leakage from mammalian membrane-mimetic EYPC/cholesterol (10: 1, w/w) liposome, but SMAP-18 and SMAP-18-W displayed 11% and 40% dye leakage. These results suggested that SMAP-18 is more selective to bacterial membranes as compared to SMAP-29 and SMAP-18-W.

Next, we measured the effects of the peptides on bacterial membrane potential in *Staphylococcus aureus* using a membrane potential sensitive dye, diSC<sub>3-5</sub>. The diSC<sub>3-5</sub> release assay indicated the peptides ability to disrupt the membrane potential across the cytoplasmic membrane. SMAP-29 and SMAP-18-W induced a significant

membrane depolarization at 1 or 2 × MIC. In contrast, SMAP-18 caused no membrane depolarization even at 4 × MIC. Our previous study, buforin-2 also induced less or no membrane depolarization even at 4 × MIC [45]. This high membrane depolarization ability of SMAP-18-W is not extended to ability to induce calcium leakage from LUVs. This may be due to reasons that SMAP-18-W could form pores on the membrane which could only allow small ions not large molecules such as calcium.

The ability of the peptides to permeabilize the outer membrane was observed using NPN uptake on *E. coli*. Increase in NPN fluorescence was due to outer membrane disintegration from peptide permeabilization. Like LL-37 and melittin, SMAP-29 was able to induce NPN uptake. However, SMAP-18 and SMAP-18-W induced relatively little NPN uptake even at 16 μM. Furthermore, the potential of inner membrane permeation of the peptides was evaluated by ONPG hydrolysis assay. Interestingly, the inner membrane permeabilizing activity of SMAP-29 is considerably higher than that of other membrane-targeting AMPs such as LL-37. However, SMAP-18 and SMAP-18-W did not induce inner membrane permeation even at 16 μM. The membrane-targeting AMPs in general have faster time-kill kinetics compared to intracellular-targeting AMPs. The time-killing kinetics of SMAP-29, SMAP-18 and SMAP-18-W were carried out using *E. coli* and *S. aureus* to compare the time taken to kill bacteria. The fast kinetics of SMAP-29 and SMAP-18-W compared to SMAP-18 indicated that the membrane as their target. On the contrary, the slow kinetics of SMAP-18 suggested that it has a different mode of interaction with the lipid bilayer. The slower killing of SMAP-18 may be due to its plausible intracellular targets.

For the determination of site of action of the peptides, FITC-labeled peptides were incubated with log phase *E. coli* and their localization was visualized by confocal

laser-scanning microscopy. Like buforin-2, it was observed that SMAP-18 was able to traverse bacterial membrane along with cell damage. This finding indicates that the major site of action of SMAP-18 is the cytoplasm of bacteria. In contrast, SMAP-29 and SMAP-18-W was unable to translocate the bacterial membrane.

The structure of SMAP-29 has three segments; the flexible N-terminal region, a hinge of Gly, nearly  $\alpha$ -helical segment of Arg 8 to Tyr 17, another hinge of glycine and proline, and  $\alpha$ -helix like carboxy-terminal region. A previous study had shown that the removal of second hinge region and carboxy-terminal region will significantly reduce the hemolytic activity [8]. It suggests that the membrane interaction is due to carboxy-terminal region following the initial electrostatic interaction of N-terminal region.

On the other hand, SMAP-18 lacks the hinge and second helix like region, thus unable to disrupt the membrane immediately as its parent peptide SMAP-29. Other studies had shown that the derivatives of SMAP-18 have amphipathic  $\alpha$ -helical structure [46]. Amphipathic  $\alpha$ -helical peptides that are rich in Arg and Leu were shown to have cell penetrating abilities without pore formation [47,48]. Thus, it is possible that SMAP-18 has a unique cell penetrating property across the membrane and killing bacteria by acting on intracellular targets.

Based on these results, we propose here that SMAP-29 and SMAP-18-W kill microorganisms by disrupting/perturbing the lipid bilayer (carpet-like model) and forming pore/ion channels on bacterial cell membranes (barrel stave model or toroidal model), respectively. In contrast, the bacterial killing SMAP-18 may be due to the inhibition of the intracellular functions (*e.g.* DNA, RNA or protein).

**Table 1.** Amino acid sequences, calculated and observed molecular masses of SMAP-29, SMAP-18 and its analogs

Peptides	Amino acid sequences	Molecular MS	
		Calculated	Measured <sup>a</sup>
SMAP-29	RGLRRLGRKIAHG $\text{VKKYGPTVLRIRIA-NH}_2$	3197.9	3197.3
SMAP-18	RGLRRLGRKIAHG $\text{VKKYG-NH}_2$	2064.5	2065.1
SMAP-18-W	RGWRRWGRKWAHG $\text{WKKYG-NH}_2$	2370.7	2371.2

**Table 2.** Antimicrobial and hemolytic activities and cell selectivity (therapeutic index) of SMAP-29, SMAP-18 and SMAP-18-W

Peptide	Minimal Inhibitory Concentration (MIC) <sup>a</sup> (μM)					GM <sup>b</sup> (μM)	HC <sub>50</sub> <sup>c</sup> (μM)	TI <sup>d</sup> (HC <sub>50</sub> /GM)
	Gram-negative bacteria			Gram-positive bacteria				
	<i>E. coli</i>	<i>P. aeruginosa</i>	<i>S. typhimurium</i>	<i>S. epidermidis</i>	<i>S. aureus</i>			
SMAP-29	2	2	1	1	1	1.4	86	61.4
SMAP-18	8	8	2	2	4	4.8	> 400	> 83.3 <sup>e</sup>
SMAP-18-W	4	8	2	2	4	4.0	> 400	>100.0 <sup>e</sup>
LL-37	8	8	4	64	8	18.4	ND <sup>f</sup>	ND
Melittin	4	8	4	4	2	4.4	ND	ND
Vancomycin	32	4	32	32	0.5	20.1	ND	ND

<sup>a</sup> The lowest peptide concentration that causes 100% inhibition of microbial growth.

<sup>b</sup> The geometric mean of MICs(minimal inhibitory concentrations)from five bacterial strains.

<sup>c</sup> The lowest peptide concentration that produces 50% hemolysis.

<sup>d</sup> Therapeutic index: The ratio of the HC<sub>50</sub>(μM) to the GM (μM).

<sup>e</sup> The “>” denotes that there were no HC<sub>50</sub> values to calculate the TI within the concentration range tested, so the reported values were minimal TI calculated with 400 μM.

<sup>f</sup> ND: not determined

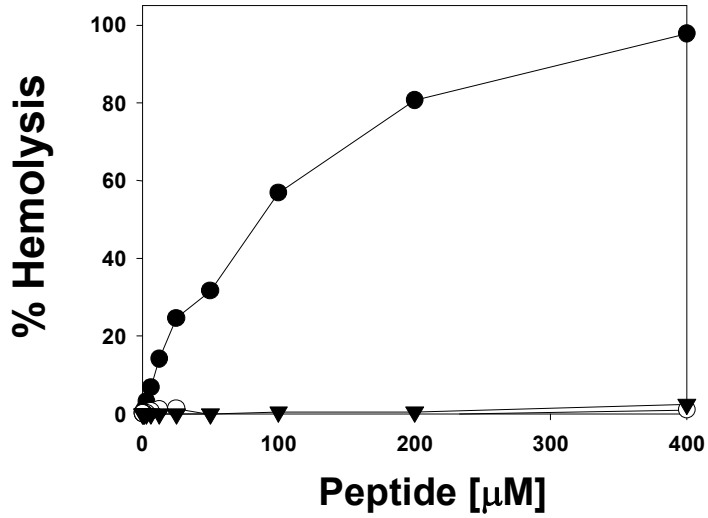


**Figure 1.** Concentration–response curves of percent hemolysis of SMAP-29, SMAP-18 and SMAP-18-W against human red blood cells. Symbols: SMAP-29 (●), SMAP-18 (○) and SMAP-18-W (▼).

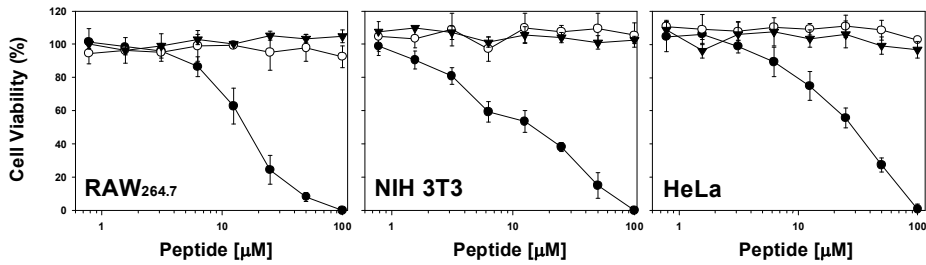


**Figure 2.** Cytotoxicity of SMAP-29, SMAP-18 and SMAP-18-W against three different types of mammalian cells, mouse macrophage RAW 264.7 cells, and mouse fibroblast NIH-3T3 cells and human cervical carcinoma HeLa cells. Symbols: SMAP-29 (●), SMAP-18 (○) and SMAP-18-W (▼).



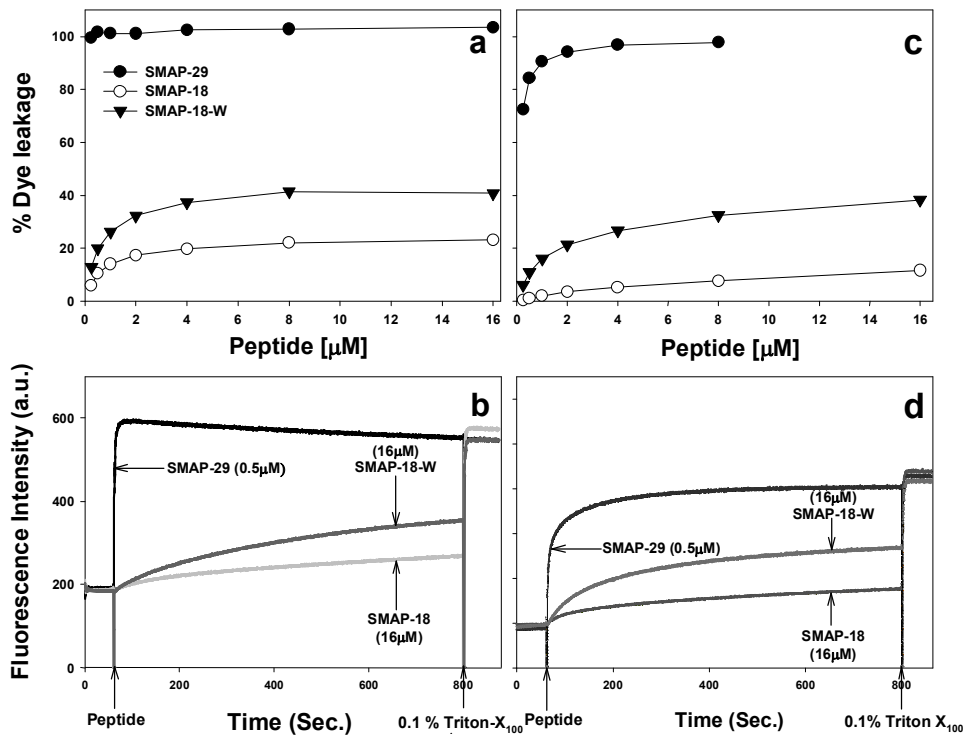


**Figure 3.**(a) Concentration-dependent peptide-induced calcein release from calcein-entrapped negatively charged EYPE/EYPG (7:3, w/w) LUVs. Symbols: SMAP-29 (●), SMAP-18 (○) and SMAP-18-W (▼). (b) Time-dependent peptide-induced calcein release from calcein-entrapped negatively charged EYPE/EYPG (7:3, w/w) LUVs.(c) Concentration-dependent peptide-induced dye release from calcein-entrapped zwitterionic EYPC/cholesterol (10: 1, w/w) LUVs. Symbols: SMAP-29 (●), SMAP-18 (○) and SMAP-18-W (▼). (d) Time-dependent peptide-induced dye release from calcein-entrapped zwitterionic EYPC/cholesterol (10: 1, w/w).

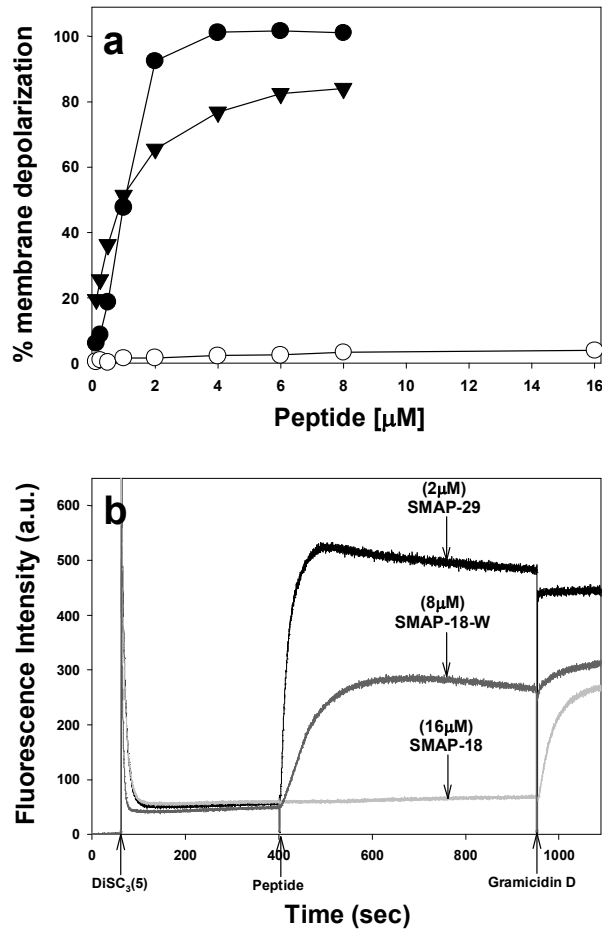


**Figure 7.**(a) Concentration-dependent membrane depolarization of *Staphylococcus aureus* by SMAP-29, SMAP-18 and SMAP-18-W. Symbols: SMAP-29 (●), SMAP-18 (○) and SMAP-18-W (▼). (b) Time-dependent membrane depolarization of *Staphylococcus aureus* by SMAP-29 (2  $\mu\text{M}$ ), SMAP-18 (16  $\mu\text{M}$ ) and SMAP-18-W (8  $\mu\text{M}$ ).

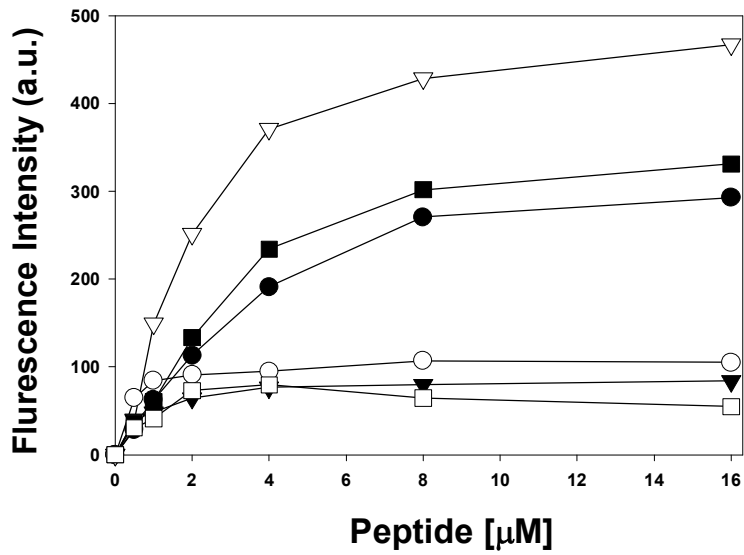


**Figure 5.** Peptide-mediated NPN uptake in *Escherichia coli*. *E.coli* cells were incubated with NPN in the presence of various concentrations of the peptides. Enhanced uptake of NPN was measured by an increase in fluorescence caused by partitioning of NPN into the hydrophobic interior of the outer membrane. Symbols: SMAP-29 (●), SMAP-18 (○), SMAP-18-W (▼), LL-37 (▽), melittin (■) and buforin-2 (□).

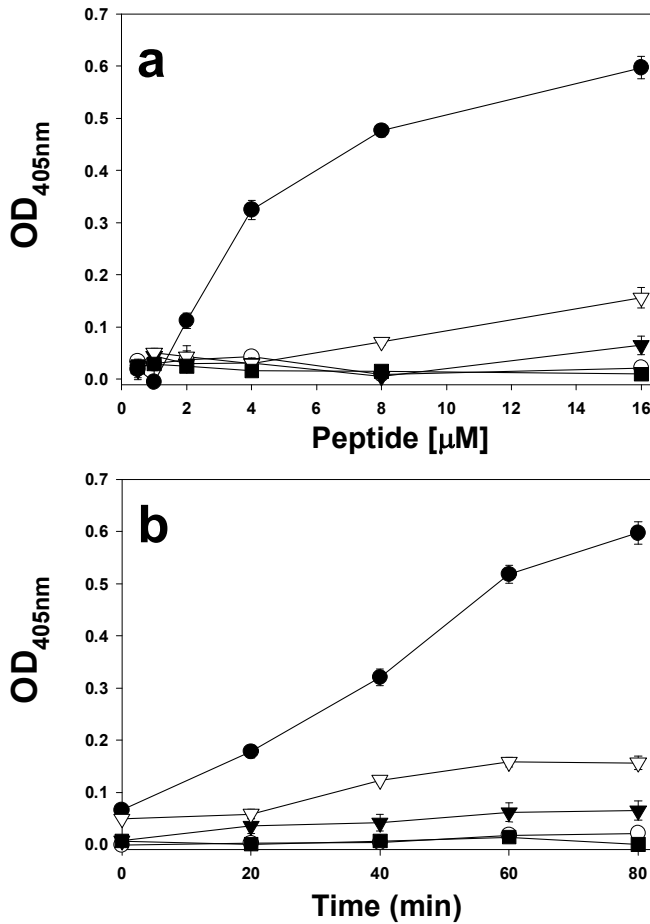


**Figure 6.** Peptide-mediated inner membrane permeabilization of *Escherichia coli* ML-35. Permeabilization was determined by following spectrophotometrically at 420 nm, the unmasking of cytoplasmic  $\beta$ -galactosidase activity as assessed by hydrolysis of the normally impermeable, chromogenic substrate ONPG. *E.coli* (approximately  $10^6$  colony forming units/ml) were resuspended in 10 mM sodium phosphate buffer, pH 7.5, containing 100mM NaCl and 1.5mM substrate. Symbols: SMAP-29 (●), SMAP-18 (○), SMAP-18-W (▼), LL-37 (▽) and buforin-2 (■).

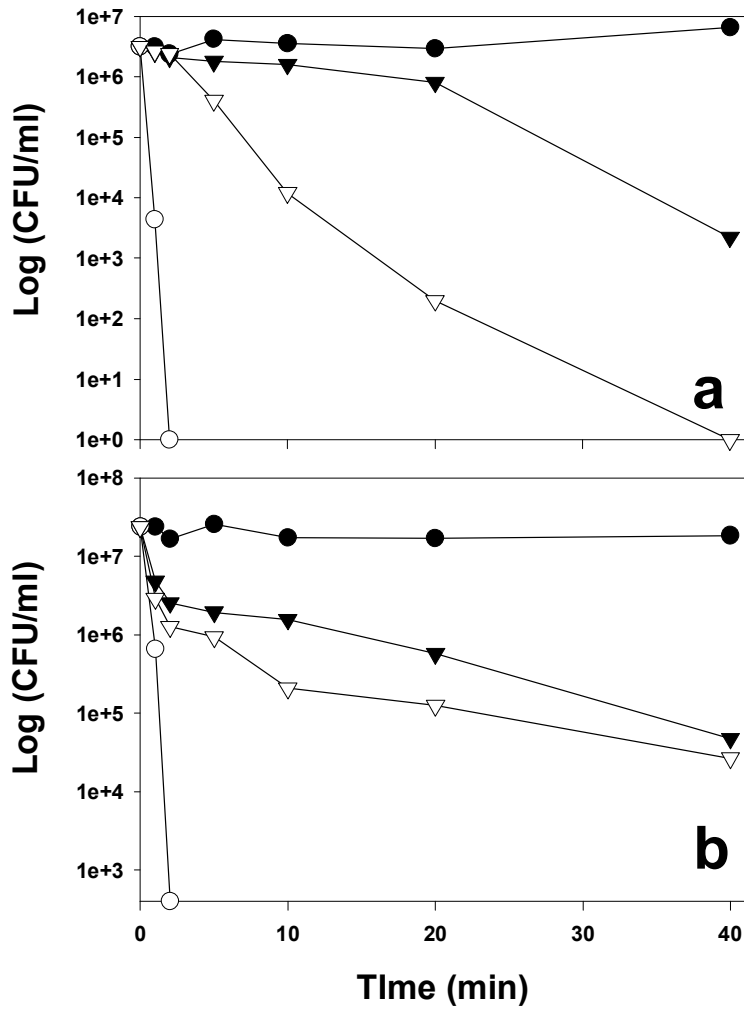


**Figure 7.** Time-kill kinetics of *Escherichia coli* (a) and *Staphylococcus aureus* (b) treated with the peptides at 0.5 × MIC. Symbols: without peptide (●), SMAP-29 (○), SMAP-18 (▼) and SMAP-18-W (▽).

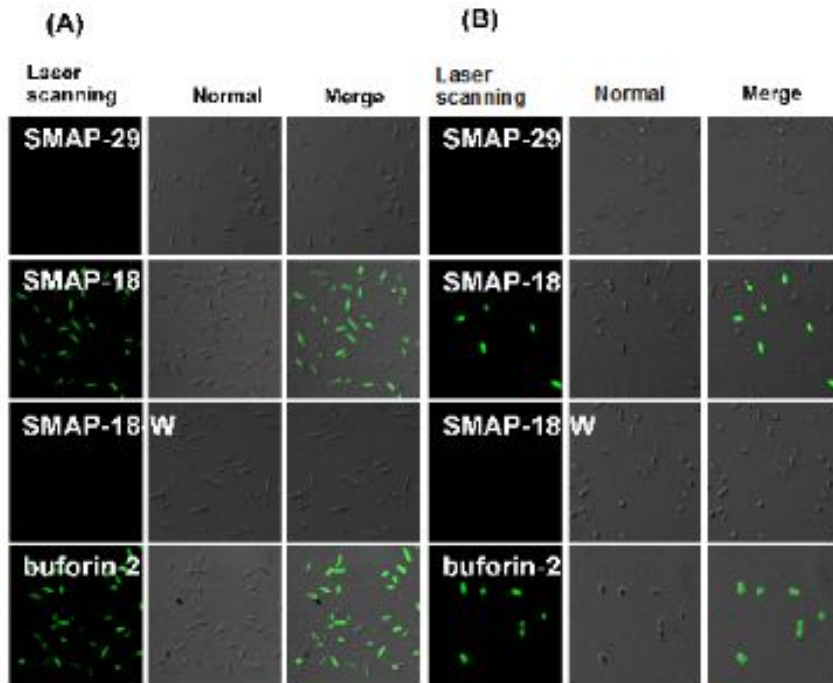


**Figure 8.** Confocal laser scanning microscopy of *Escherichia coli* (KCTC 1682) or *Staphylococcus aureus* (KCTC 1621) treated with FITC-labeled peptides. The cells were incubated with FITC-labeled peptides (5  $\mu\text{g/ml}$ ) at 37  $^{\circ}\text{C}$  for 30 min. Panels on the left, middle and right represent laser-scanning images, transmitted light scanning image (normal image), and merged image of *E. coli* (A) and *S. aureus* (B) respectively, treated with FITC-labeled peptides.

## 5. References

- [1] J. Turner, Y. Cho, N.N. Dinh, A.J. Waring, R.I. Lehrer, Activities of LL-37, a cathelin-associated antimicrobial peptide of human neutrophils., *Antimicrob. Agents Chemother.* 42 (1998) 2206–14.
- [2] R. Gennaro, M. Zanetti, Structural features and biological activities of the cathelicidin-derived antimicrobial peptides., *Biopolymers.* 55 (2000) 31–49. doi:10.1002/1097-0282(2000)55:1<31::AID-BIP40>3.0.CO;2-9.
- [3] S.M. Travis, N.N. Anderson, W.R. Forsyth, C. Espiritu, B.D. Conway, E.P. Greenberg, et al., Bactericidal activity of mammalian cathelicidin-derived peptides., *Infect. Immun.* 68 (2000) 2748–55.
- [4] M. Zanetti, R. Gennaro, D. Romeo, Cathelicidins: a novel protein family with a common proregion and a variable C-terminal antimicrobial domain., *FEBS Lett.* 374 (1995) 1–5.
- [5] L. Bagella, M. Scocchi, M. Zanetti, cDNA sequences of three sheep myeloid cathelicidins., *FEBS Lett.* 376 (1995) 225–8.
- [6] R.M. Dawson, C.-Q. Liu, Cathelicidin peptide SMAP-29: comprehensive review of its properties and potential as a novel class of antibiotics, *Drug Dev. Res.* 70 (2009) 481–498. doi:10.1002/ddr.20329.
- [7] B. Skerlavaj, M. Benincasa, A. Risso, M. Zanetti, R. Gennaro, SMAP-29: a potent antibacterial and antifungal peptide from sheep leukocytes, *FEBS Lett.* 463 (1999) 58–62. doi:10.1016/S0014-5793(99)01600-2.
- [8] S.Y. Shin, E.J. Park, S.T. Yang, H.J. Jung, S.H. Eom, W.K. Song, et al., Structure-activity analysis of SMAP-29, a sheep leukocytes-derived antimicrobial peptide., *Biochem. Biophys. Res. Commun.* 285 (2001) 1046–51. doi:10.1006/bbrc.2001.5280.
- [9] R.M. Dawson, C.-Q. Liu, Analogues of peptide SMAP-29 with comparable antimicrobial potency and reduced cytotoxicity., *Int. J. Antimicrob. Agents.* 37 (2011) 432–7. doi:10.1016/j.ijantimicag.2011.01.007.
- [10] W. Hu, K.C. Lee, T.A. Cross, Tryptophans in membrane proteins: indole ring orientations and functional implications in the gramicidin channel., *Biochemistry.* 32 (1993) 7035–47.
- [11] D. Oh, S.Y. Shin, S. Lee, J.H. Kang, S.D. Kim, P.D. Ryu, et al., Role of the hinge region and the tryptophan residue in the synthetic antimicrobial peptides,

- cecropin A(1-8)-magainin 2(1-12) and its analogues, on their antibiotic activities and structures., *Biochemistry*. 39 (2000) 11855–64.
- [12] K. Park, D. Oh, S.Y. Shin, K.-S. Hahm, Y. Kim, Structural studies of porcine myeloid antibacterial peptide PMAP-23 and its analogues in DPC micelles by NMR spectroscopy., *Biochem. Biophys. Res. Commun.* 290 (2002) 204–12. doi:10.1006/bbrc.2001.6173.
- [13] M. Stark, L.-P. Liu, C.M. Deber, Cationic hydrophobic peptides with antimicrobial activity., *Antimicrob. Agents Chemother.* 46 (2002) 3585–90.
- [14] D.A. Scudiero, R.H. Shoemaker, K.D. Paull, A. Monks, S. Tierney, T.H. Nofziger, et al., Evaluation of a soluble tetrazolium/formazan assay for cell growth and drug sensitivity in culture using human and other tumor cell lines., *Cancer Res.* 48 (1988) 4827–33.
- [15] M. Wu, E. Maier, R. Benz, R.E. Hancock, Mechanism of interaction of different classes of cationic antimicrobial peptides with planar bilayers and with the cytoplasmic membrane of *Escherichia coli*., *Biochemistry*. 38 (1999) 7235–42. doi:10.1021/bi9826299.
- [16] C.L. Friedrich, D. Moyles, T.J. Beveridge, R.E. Hancock, Antibacterial action of structurally diverse cationic peptides on gram-positive bacteria., *Antimicrob. Agents Chemother.* 44 (2000) 2086–92.
- [17] B. Loh, C. Grant, R.E. Hancock, Use of the fluorescent probe 1-N-phenyl-naphthylamine to study the interactions of aminoglycoside antibiotics with the outer membrane of *Pseudomonas aeruginosa*., *Antimicrob. Agents Chemother.* 26 (1984) 546–51.
- [18] R.E. Hancock, S.W. Farmer, Mechanism of uptake of deglucoteicoplanin amide derivatives across outer membranes of *Escherichia coli* and *Pseudomonas aeruginosa*., *Antimicrob. Agents Chemother.* 37 (1993) 453–6.
- [19] S. Ono, S. Lee, Y. Kodera, H. Aoyagi, M. Waki, T. Kato, et al., Environment-dependent conformation and antimicrobial activity of a gramicidin S analog containing leucine and lysine residues., *FEBS Lett.* 220 (1987) 332–6.
- [20] R.I. Lehrer, A. Barton, K.A. Daher, S.S. Harwig, T. Ganz, M.E. Selsted, Interaction of human defensins with *Escherichia coli*. Mechanism of bactericidal activity., *J. Clin. Invest.* 84 (1989) 553–61. doi:10.1172/JCI114198.
- [21] B. Skerlavaj, D. Romeo, R. Gennaro, Rapid membrane permeabilization and inhibition of vital functions of gram-negative bacteria by bactenecins., *Infect. Immun.* 58 (1990) 3724–30.



- [22] J.Y. Lee, S.-T. Yang, S.K. Lee, H.H. Jung, S.Y. Shin, K.-S. Hahm, et al., Salt-resistant homodimeric bactenecin, a cathelicidin-derived antimicrobial peptide., *FEBS J.* 275 (2008) 3911–20. doi:10.1111/j.1742-4658.2008.06536.x.
- [23] J.-J. Koh, S. Qiu, H. Zou, R. Lakshminarayanan, J. Li, X. Zhou, et al., Rapid bactericidal action of alpha-mangostin against MRSA as an outcome of membrane targeting., *Biochim. Biophys. Acta.* 1828 (2013) 834–44. doi:10.1016/j.bbamem.2012.09.004.
- [24] Y. Chen, C.T. Mant, S.W. Farmer, R.E.W. Hancock, M.L. Vasil, R.S. Hodges, Rational design of alpha-helical antimicrobial peptides with enhanced activities and specificity/therapeutic index., *J. Biol. Chem.* 280 (2005) 12316–29. doi:10.1074/jbc.M413406200.
- [25] M.A. Fázio, L. Jouvensal, F. Vovelle, P. Bulet, M.T.M. Miranda, S. Daffre, et al., Biological and structural characterization of new linear gomesin analogues with improved therapeutic indices, *Biopolym. - Pept. Sci. Sect.* 88 (2007) 386–400.
- [26] K.H. Park, Y. Park, I.-S. Park, K.-S. Hahm, S.Y. Shin, Bacterial selectivity and plausible mode of antibacterial action of designed Pro-rich short model antimicrobial peptides., *J. Pept. Sci.* 14 (2008) 876–82. doi:10.1002/psc.1019.
- [27] C. Solanas, B.G. de la Torre, M. Fernández-Reyes, C.M. Santiveri, M.A. Jiménez, L. Rivas, et al., Therapeutic index of gramicidin S is strongly modulated by D-phenylalanine analogues at the beta-turn., *J. Med. Chem.* 52 (2009) 664–74. doi:10.1021/jm800886n.
- [28] K.H. Park, Y.H. Nan, Y. Park, J. Il Kim, I.-S. Park, K.-S. Hahm, et al., Cell specificity, anti-inflammatory activity, and plausible bactericidal mechanism of designed Trp-rich model antimicrobial peptides., *Biochim. Biophys. Acta.* 1788 (2009) 1193–203. doi:10.1016/j.bbamem.2009.02.020.
- [29] Y.H. Nan, J.K. Bang, B. Jacob, I.S. Park, S.Y. Shin, Prokaryotic selectivity and LPS-neutralizing activity of short antimicrobial peptides designed from the human antimicrobial peptide LL-37, *Peptides.* 35 (2012) 239–247.
- [30] K. Matsuzaki, Magainins as paradigm for the mode of action of pore forming polypeptides., *Biochim. Biophys. Acta.* 1376 (1998) 391–400.
- [31] Z. Oren, Y. Shai, Mode of action of linear amphipathic alpha-helical antimicrobial peptides., *Biopolymers.* 47 (1998) 451–63. doi:10.1002/(SICI)1097-0282(1998)47:6<451::AID-BIP4>3.0.CO;2-F.

- [32] W.T. Heller, A.J. Waring, R.I. Lehrer, T.A. Harroun, T.M. Weiss, L. Yang, et al., Membrane thinning effect of the beta-sheet antimicrobial protegrin., *Biochemistry*. 39 (2000) 139–45.
- [33] A. Giuliani, G. Pirri, A. Bozzi, A. Di Giulio, M. Aschi, A.C. Rinaldi, Antimicrobial peptides: natural templates for synthetic membrane-active compounds., *Cell. Mol. Life Sci.* 65 (2008) 2450–60. doi:10.1007/s00018-008-8188-x.
- [34] L.T. Nguyen, E.F. Haney, H.J. Vogel, The expanding scope of antimicrobial peptide structures and their modes of action., *Trends Biotechnol.* 29 (2011) 464–72. doi:10.1016/j.tibtech.2011.05.001.
- [35] H. Sato, J.B. Feix, Peptide-membrane interactions and mechanisms of membrane destruction by amphipathic alpha-helical antimicrobial peptides., *Biochim. Biophys. Acta.* 1758 (2006) 1245–56. doi:10.1016/j.bbamem.2006.02.021.
- [36] L. Zhang, A. Rozek, R.E. Hancock, Interaction of cationic antimicrobial peptides with model membranes., *J. Biol. Chem.* 276 (2001) 35714–22. doi:10.1074/jbc.M104925200.
- [37] D. Allende, S.A. Simon, T.J. McIntosh, Melittin-induced bilayer leakage depends on lipid material properties: evidence for toroidal pores., *Biophys. J.* 88 (2005) 1828–37. doi:10.1529/biophysj.104.049817.
- [38] J.T.J. Cheng, J.D. Hale, M. Elliot, R.E.W. Hancock, S.K. Straus, Effect of membrane composition on antimicrobial peptides aurein 2.2 and 2.3 from Australian southern bell frogs., *Biophys. J.* 96 (2009) 552–65. doi:10.1016/j.bpj.2008.10.012.
- [39] A.S. Ladokhin, S.H. White, “Detergent-like” permeabilization of anionic lipid vesicles by melittin., *Biochim. Biophys. Acta.* 1514 (2001) 253–60.
- [40] G. Wiedman, K. Herman, P. Searson, W.C. Wimley, K. Hristova, The electrical response of bilayers to the bee venom toxin melittin: evidence for transient bilayer permeabilization., *Biochim. Biophys. Acta.* 1828 (2013) 1357–64. doi:10.1016/j.bbamem.2013.01.021.
- [41] C.B. Park, H.S. Kim, S.C. Kim, Mechanism of action of the antimicrobial peptide buforin II: buforin II kills microorganisms by penetrating the cell membrane and inhibiting cellular functions., *Biochem. Biophys. Res. Commun.* 244 (1998) 253–7. doi:10.1006/bbrc.1998.8159.
- [42] C.B. Park, K.S. Yi, K. Matsuzaki, M.S. Kim, S.C. Kim, Structure-activity analysis of buforin II, a histone H2A-derived antimicrobial peptide: the proline

- hinge is responsible for the cell-penetrating ability of buforin II., *Proc. Natl. Acad. Sci. U. S. A.* 97 (2000) 8245–50. doi:10.1073/pnas.150518097.
- [43] S. Kobayashi, A. Chikushi, S. Tougu, Y. Imura, M. Nishida, Y. Yano, et al., Membrane translocation mechanism of the antimicrobial peptide buforin 2., *Biochemistry.* 43 (2004) 15610–6. doi:10.1021/bi048206q.
- [44] Y.M. Song, Y. Park, S.S. Lim, S.-T. Yang, E.-R. Woo, I.-S. Park, et al., Cell selectivity and mechanism of action of antimicrobial model peptides containing peptoid residues., *Biochemistry.* 44 (2005) 12094–106. doi:10.1021/bi050765p.
- [45] W.L. Zhu, K.-S. Hahm, S.Y. Shin, Cell selectivity and mechanism of action of short antimicrobial peptides designed from the cell-penetrating peptide Pep-1., *J. Pept. Sci.* 15 (2009) 569–75. doi:10.1002/psc.1145.
- [46] M. V Sawai, A.J. Waring, W.R. Kearney, P.B. McCray, W.R. Forsyth, R.I. Lehrer, et al., Impact of single-residue mutations on the structure and function of ovispirin/novispirin antimicrobial peptides., *Protein Eng.* 15 (2002) 225–32.
- [47] A. Walrant, A. Vogel, I. Correia, O. Lequin, B.E.S. Olausson, B. Desbat, et al., Membrane interactions of two arginine-rich peptides with different cell internalization capacities., *Biochim. Biophys. Acta.* 1818 (2012) 1755–63. doi:10.1016/j.bbamem.2012.02.024.
- [48] D. Derossi, G. Chassaing, A. Prochiantz, Trojan peptides: the penetratin system for intracellular delivery., *Trends Cell Biol.* 8 (1998) 84–7.

## **PART III**

**Enantiomer and diastereomers of sheep myeloid antimicrobial peptide-29 (SMAP-29) with improved cell selectivity and different membrane interaction**

## 1. Introduction

Antimicrobial peptides (AMPs) are often regarded as promising alternatives to the increasingly ineffective conventional antibiotics. They are additionally attractive for therapeutics use because of their ability for immune modulation, including anti-inflammatory action. Another desirable quality of AMP as drugs is less chance of side reaction. Despite all these well-disposed traits, AMPs suffer some drawbacks to be used as drug; cytotoxicity, poor biostability and lower activity, and higher size are being the major disadvantages [1–5].

Lipopolysaccharide (LPS)-induced inflammation is a serious threat associated with Gram- negative infection, which still lacks any complete effective treatment. This is amplified by the emergence of drug resistance. Thus, an ideal antibacterial drug should have both bactericidal action and anti-endotoxin effects [6,7]. Many AMPs have LPS-neutralizing properties combined with relatively higher efficiency against drug resistant pathogens, making them as ideal drug candidate for this double jeopardy. Intense research had been done on how to modify the properties of AMPs, enhancing the good qualities while eliminating or improving the undesirable properties [8,9].

Sheep myeloid antimicrobial peptide-29 (SMAP-29) belongs to the cathelicidin family of AMPs. However, SMAP-29 is equally cytotoxic to host cells, making them difficult to consider for antibiotics [10,11]. SMAP-29 had  $\alpha$ -helical N-terminal, hinge and a heavily hydrophobic C-terminal. The hinge region is induced by glycine and proline at 18<sup>th</sup> and 19<sup>th</sup> positions [12]. It had been showed that trimming SMAP-29 at this point will remove its cytotoxicity, while retaining the antimicrobial activity [13].

Isoleucine has a second asymmetric carbon center at carbon position 3 along its chain. Therefore, isoleucine has four configurations in R/S notation. The absolute configuration of the normal protein component, L-isoleucine, is 2S,3S. D-isoleucine is 2R,3R-configuration. The diastereomer with 2R, 3S-configuration is D-allo-isoleucine. Previous study had showed that AMP, Pin 2 (FWGALAKGALKLIPSLFSSFSKGD) from African scorpion *Pandinus imperator* and its D-Pin2 with D-allo-isoleucine had different retention time in analytical RP-HPLC profile [14]. D-form of some AMPs containing D-allo-isoleucine has different interaction with membrane compared to

corresponding L-form [15,16].

In the present study, in order to investigate the effects of L- to D-amino acid conversion of SMAP-29 on the structure, membrane interaction, cell selectivity (bacterial cells versus mammalian cells) and LPS-neutralizing activity, we synthesized SMAP-29 and its SMAP-29D (the enantiomer) with D-isoleucine (2R, 3R-configuration) and SMAP-29DA (the diastereomer) with D-allo-isoleucine (2R, 3S-configuration). SMAP-29 has antimicrobial and LPS-neutralizing properties [12,17]. It was clear from previous studies that the C-terminal amino acids largely contribute to cytotoxicity of this peptide [13,18]. In this study, in order to reduce the cytotoxicity of SMAP-29 without losing antimicrobial and LPS-neutralizing activities, and to investigate the effect of introduction of D-amino acids at C-terminal region of SMAP-29 on cell selectivity and LPS-neutralizing activity, we synthesized two diastereomers (SMAP-29HD and SMAP-29HDA). These two peptides have 1-18 residues of L-amino acids and D-amino acid substitution in 19-28 residues with D-isoleucine and D-allo-isoleucine are replaced in SMAP-29HD and SMAP-29HDA, respectively.

Although the mechanism of action of AMPs has not been clarified, it is believed that most AMPs kill bacteria by disrupting/perturbing the lipid bilayer and forming pore/ion channels on bacterial cell membranes (*i.e.*, membrane-targeting AMPs). In contrast, a few AMPs such as buforin 2, PR-39 and Bac 7 were known to penetrate microbial cell membranes without inducing membrane permeabilization and cause bacterial cell death by inhibiting protein, DNA or RNA synthesis (*i.e.*, intracellular-targeting AMPs) [19]. In previous work, we reported that SMAP-18 corresponding to N-terminal fragment (1-18 residues) of SMAP-29 has the intracellular targeting-mechanism. SMAP-18 is non-disruptive to the bacterial membrane while the parent molecule SMAP-29 is acting on the lipid bilayer [18]. The interaction of SMAP-29 with mammalian cell membranes is due to the hydrophobic interaction of between hydrophobic residues and the core of lipid bilayer. SMAP-18, which lacks this lining of hydrophobic amino acids in the carboxyl side of SMAP-29, did not induce any membrane perturbation. This led us to study the nature of hydrophobic interaction of SMAP-29 with lipid bilayer.

Most studies have shown that D-enantiomers of membrane-targeting AMPs have similar antimicrobial activity *in vitro* to their L-enantiomers. This suggests that the

antimicrobial mechanism of these AMPs does not involve stereoselective interactions with chiral enzymes, lipids or protein receptors. In this study, to examine the antimicrobial activity and the ability to traverse through the bacterial membrane of D-enantiomer of intracellular-targeting AMP compared to its L-enantiomer, we had prepared D-enantiomers of SMAP-18 (SMAP-18D and SMAP-18DA) with D-amino acid substitution. Here, D-isolucine and D-allo-isolucine are located in SMAP-18D and SMAP-18DA, respectively. It is well established that our designed enantiomers and diastereomers of SMAP-29 and SMAP-18 composed of D-amino acid are resistant to both bacterial proteases as well as host proteases [14,20].

## 2. Materials and methods

### 2.1 Materials

Rink amide 4-methylbenzhydrylamine (MBHA) resin, 9-fluorenylmethoxycarbonyl (Fmoc) amino acids and Fmoc-D-allo-Ile-OH were obtained from Calbiochem-Novabiochem (La Jolla, CA, USA). Fmoc-D-Ile-OH had purchased from Bachem (Bachem AG, Bubendorf), other reagents used for peptide synthesis are obtained from, TFA (Sigma, St. Louis, MO, USA), piperidine (Merck, Darmstadt, Germany), DCC (Fluka, Buchs, Switzerland), HOBt (Aldrich) and DMF (peptide synthesis grade; Biolab). DiSC<sub>3</sub>-5 was obtained from Molecular Probes (Eugene, OR, USA). EYPE, EYPG, EYPC, gramicidin D, calcein by Sigma Chemical Co. (St. Louis, MO, USA). DMEM and FBS were supplied by HyClone (SeouLin, Bioscience, Korea) and Lonza (Lonza Walkerville Inc.), respectively. All other reagents were of analytical grade. The buffers were prepared in double glass-distilled water.

### 2.2 Peptide Synthesis

All peptides were synthesized by the standard Fmoc-based solid-phase method on rink amide 4-methylbenzhydrylamine resin. DCC and HOBt were used as coupling reagents, and fivefold excess Fmoc-amino acids were added during every coupling cycle. After cleavage and deprotection with a mixture of TFA/water/thioanisole/phenol/ethanedithiol/triisopropylsilane (81.5 : 5 : 5 : 5 : 2.5:1, v/v/v/v/v) for 2 h at room temperature, the crude peptide was repeatedly extracted with diethyl ether and purified by RP-HPLC on a preparative Vydac C18 column (20 mm ×250 mm, 300 Å, 15-mm particle size) using an appropriate 0–90% water/acetonitrile gradient in the presence of 0.05% TFA. The final purity of the peptides (>95%) was assessed by RP-HPLC on an analytical Vydac C<sub>18</sub> column (4.6 ×250 mm, 300 Å, 5-mm particle size). The molecular mass of synthetic peptides was determined by MALDI-TOF MS (Shimadzu, Kyoto, Japan) (Table 1).

### 2.3 Circular Dichroism (CD) Spectroscopy

The CD spectrum of the peptide was obtained with a Jasco J-715 CD spectrophotometer



(Tokyo, Japan) at 25 °C using a fused quartz cell with a 1-mm path length over a wavelength range of 190–250 nm at 0.1 nm intervals (speed, 50 nm/min; response time, 0.5 s; bandwidth, 1 nm). CD spectra were collected and averaged over two scans. Samples were prepared by dissolving the peptide to a final concentration of 100 µg/ml in 10mM sodium phosphate buffer (pH7.2), 30mM SDS or 0.1% LPS. The mean residue ellipticity  $[\theta]$ , was given in degree  $\cdot\text{cm}^2\cdot\text{dmol}^{-1}$ . The spectra were expressed as molar ellipticity  $[\theta]$  vs. wavelength.

## 2.4 Antimicrobial Assay

### 2.4.1 Broth microdilution method

The antimicrobial activity of the peptides against bacteria had examined by using the broth microdilution method in sterile 96-well plates. Aliquots (100 µl) of a bacterial suspension at  $2 \times 10^6$  CFU/ml in 1% peptone were added to 100 µl of the peptide solution (serial 2-fold dilutions in 1% peptone). After incubation for 18–20 h at 37°C, bacterial growth inhibition was determined by measuring the absorbance at 600 nm with a Microplate Autoreader EL 800 (Bio-Tek Instruments, VT). The minimal inhibitory concentration (MIC) was defined as the lowest peptide concentration that causes 100% inhibition of microbial growth. Two types of Gram-positive bacteria (*Staphylococcus epidermidis* [KCTC 1917] and *Staphylococcus aureus* [KCTC 1621]) and three types of Gram-negative bacteria (*Escherichia coli* [KCTC 1682], *Pseudomonas aeruginosa* [KCTC 1637] and *Salmonella typhimurium* [KCTC 1926]) were procured from the Korean Collection for Type Cultures (KCTC) at the Korea Research Institute of Bioscience and Biotechnology (KRIBB).

### 2.4.2 Agar Plate Disc Diffusion Method

For SMAP-18L and SMAP-18D peptides, MIC was additionally determined using agar plate disc diffusion method. Agar plates were prepared by inoculating  $2 \times 10^5$  CFU/mL of *E.coli* to 2.5% LB broth and 0.8% agar mixture and allowed to solidify. Peptides diluted to 10µL were added to the paper discs and incubated at 37°C for 1 day. The

diameter of the clear zone is manually measured and images had taken digitally.

## 2.5 Measurement of Hemolytic Activity

The hemolytic activity of the peptides was measured as the amount of hemoglobin released by the lysis of human erythrocytes [21]. Fresh human red blood cells (hRBCs) were centrifuged, washed three times with PBS (35 mM phosphate buffer, 0.15 M NaCl, pH 7.4), dispensed into 96-well plates as 100  $\mu$ l of 4% (w/v) hRBC in PBS, and 100  $\mu$ l of peptide solution was added to each well. Plates were incubated for 1 h at 37 °C, then centrifuged at 1000  $\times$  g for 5 min. Samples (100  $\mu$ l) of supernatant were transferred to 96-well plates and hemoglobin release was monitored by measuring absorbance at 414 nm. Zero hemolysis was determined in PBS ( $A_{\text{PBS}}$ ) and 100% hemolysis was determined in 0.1% (v/v) Triton X-100 ( $A_{\text{triton}}$ ). The hemolysis percentage hemolysis was calculated as: % hemolysis =  $100 \times [(A_{\text{sample}} - A_{\text{PBS}}) / (A_{\text{triton}} - A_{\text{PBS}})]$

## 2.6 Cell Culture

RAW 264.7 cells were purchased from the American Type Culture Collection (Manassas, VA) and cultured in DMEM with 10% fetal bovine serum and antibiotic-antimycotic solution (100 units/ml penicillin, 100  $\mu$ g/ml streptomycin and 25  $\mu$ g/ml amphotericin B) in 5% CO<sub>2</sub> at 37 °C. Cultures were passed every 2 to 3 days, and cells were detached by brief trypsin treatment, and visualized with an inverted microscope.

## 2.7 Cytotoxicity against Mammalian Cells

Cytotoxicity of peptides against RAW 264.7 cells was determined using the MTT proliferation assay as reported previously with minor modifications [22]. The cells were seeded on 96-well microplates at a density of  $2 \times 10^4$  cells/well in 150  $\mu$ l DMEM containing 10% fetal bovine serum. Plates were incubated for 24 h at 37 °C in 5% CO<sub>2</sub>. Peptide solutions (20  $\mu$ l) (serial 2-fold dilutions in DMEM) were added, and the plates further incubated for 2 days. Wells containing cells without peptides served as controls. Subsequently, 20  $\mu$ l MTT solution (5 mg/ml) was added in each well, and the plates were incubated for a further 4 h at 37 °C. Precipitated MTT formazan was dissolved in 40  $\mu$ l of 20% (w/v) SDS containing 0.01 M HCl for 2h. Absorbance at 570 nm was measured using Microplate reader EL 800 (Bio-Tek Instruments, VT). Cell

survival was expressed as a percentage of the ratio of  $A_{570}$  of cells treated with peptide to that of untreated cells.

### **2.8 Assays for Evaluation of LPS-neutralizing Activity**

Cultured RAW264.7 macrophage cells at  $3 \times 10^5$  cells/well in 96-well plate were stimulated with *E. coli* LPS O111:B4 (20 ng/ml) in the presence (10  $\mu$ M) or absence of peptides. Cells stimulated with LPS alone and untreated cells were used for maximum and minimum tumor necrosis factor- $\alpha$  (TNF- $\alpha$ ) production in a given set of experiments. The cells were later incubated for 12 h at 37°C in an incubator. Afterward, samples of the medium from each treatment were collected. Concentrations TNF- $\alpha$  in the samples were evaluated using mouse enzyme-linked immunosorbent assay kits for TNF- $\alpha$  (R&D Systems, Minneapolis, MN, USA) according to the manufacturers' protocol. To evaluate secreted interleukin-6 (IL-6) and MCP-1, cells are treated in same way as for TNF- $\alpha$  estimation. Afterward, samples of the medium from each treatment were collected. Concentrations IL-6 and MCP-1 in the samples were evaluated using mouse enzyme-linked immunosorbent assay kits for IL-6 and MCP-1 (R&D Systems, Minneapolis, MN, USA) according to the manufacturers' protocol.

### **2.9 Nitric oxide (NO) Production Inhibition Assay**

Nitrite accumulation in culture media was used as an indicator of nitric oxide (NO) production. Cells were plated at a density of  $3 \times 10^5$  cells ml<sup>-1</sup> in 96-well culture plates, and stimulated with LPS (20 ng/ml) from *E. coli* O111:B4 (Sigma) in the presence or absence of peptides for 24 h. Isolated supernatant fractions were mixed with an equal volume of Griess reagent (1% sulfanilamide, 0.1% naphthylethylenediamine dihydrochloride, and 2% phosphoric acid) and incubated at room temperature for 10 min. Nitrite production was measured by absorbance at 540 nm, and the concentrations were determined using a standard curve generated with NaNO<sub>2</sub>.

### **2.10 Dye Leakage Assay**

Calcein-entrapped LUVs composed of EYPE/EYPG (7:3, w/w) were prepared by vortexing the dried lipid in dye buffer solution (70 mM calcein, 10mM Tris, 150 mM

NaCl, 0.1 mM EDTA, pH 7.4). The suspension was subjected to 10 frozen-thaw cycles in liquid nitrogen and extruded 21 times through polycarbonate filters (two stacked 100-nm pore size filters) with a LiposoFast extruder (Avestin, Inc. Canada). Untrapped calcein was removed by gel filtration on a Sephadex G-50 column. The concentration of calcein-entrapped LUVs was determined by phosphorus analysis. Calcein leakage from LUVs was monitored at room temperature by measuring fluorescence intensity at an excitation wavelength of 490 nm and emission wavelength of 520 nm on a model RF-5301PC spectrophotometer. Complete dye release was obtained by using 0.1% Triton X-100.

### **2.11 Membrane Depolarization Assay**

The cytoplasmic membrane depolarization activity of the peptides was measured using the membrane potential sensitive dye, diSC<sub>3</sub>-5 as previously described [23,24]. Briefly, *Staphylococcus aureus* (KCTC 1621) grown at 37°C with agitation to the mid-log phase (OD<sub>600</sub> = 0.4) was harvested by centrifugation. Cells were washed twice with washing buffer (20 mM glucose, 5 mM HEPES, pH 7.4) and resuspended to an OD<sub>600</sub> of 0.05 in similar buffer. The cell suspension was incubated with 20 nM diSC<sub>3</sub>-5 until stable fluorescence was achieved, implying incorporation of the dye into the bacterial membrane. Then KCl was added to a final concentration of 0.1 M to equilibrate K<sup>+</sup> levels. Membrane depolarization was monitored by recording changes in the intensity of fluorescence emission of the membrane potential-sensitive dye, diSC<sub>3</sub>-5 (excitation  $\lambda$  = 622 nm, emission  $\lambda$  = 670 nm) after peptide addition. The membrane potential was fully dissipated by adding gramicidin D (final concentration of 0.2 nM).

### **2.12 DNA Binding Assay**

Gel retardation experiments were performed by mixing 100 ng of the plasmid DNA (pBluescript II SK+) with increasing amounts of peptide in 20  $\mu$ l of binding buffer (5% glycerol, 10 mM Tris-HCl, pH 8.0, 1 mM EDTA, 1 mM dithiothreitol, 20 mM KCl, and 50  $\mu$ g/ml bovine serum albumin). Reaction mixtures were incubated at room temperature for 1 h. Subsequently, 4  $\mu$ l of native loading buffer was added (10% Ficoll 400, 10 mM Tris-HCl, pH 7.5, 50 mM EDTA, 0.25% bromophenol blue, and 0.25% xylene cyanol), and a 20  $\mu$ l aliquot subjected to 1% agarose gel electrophoresis in

0.5 × Tris borate-EDTA buffer (45 mM Tris-borate and 1 mM EDTA, pH 8.0).

### 2.13 Killing Kinetics Assay

The time-killing kinetics of the peptides was assessed using *E.coli* (KCTC 1682) as described in previous studies[25]. The initial density of the cultures was approximately  $1 \times 10^6$  CFU/ml. After 1, 2, 5, 10, 20, 40 and 60 min of exposure to the peptides at 37°C, 50 µl aliquots of serial 10-fold dilutions (up to  $10^{-3}$ ) of the cultures were plated onto Luria-Bertani (LB) agar plates to obtain viability counts. Colonies were counted after incubation for 24 h at 37 °C.

## 3. Results

### 3.1 Design and Synthesis of Peptides

Isoleucine has two chiral centers, thus, it forms four different stereoisomers. The L-enantiomer (L-Ile) and D-enantiomer (D-Ile) of isoleucine has 2S, 3S- and 2R, 3R-configuration in R/S notation, respectively. The diastereomer with 2R, 3S-configuration is D-allo-isoleucine. SMAP-29 contains 4 isoleucines. In particular, 3 isoleucines exist in its C-terminal region. The C-terminal is involved in the hydrophobic interaction with lipid membrane. Since D-isoleucine and D-allo-isoleucine have different spatial orientation of their side chains, two peptide isomers composed of multiple D-isoleucine or multiple D-allo-isoleucine may have interact differently with membrane. In the present study, in order to investigate the effects of L- to D-amino acid conversion of SMAP-29 on the structure, membrane interaction, antimicrobial activity, hemolytic activity and LPS-neutralizing activity, we synthesized SMAP-29, SMAP-29D (D-enantiomer) containing D-isoleucine and SMAP-29DA (diastereomer) containing D-allo-isoleucine.

Structure-function analysis studies of SMAP-29 suggested that the C-terminal hydrophobic region (19-28 residues) is responsible for its cytotoxicity toward eukaryotic cells [13,18]. In this study, in order to examine the effect of incorporation of D-amino acids in the C-terminal region (19-28 residues) of SMAP-29 on antimicrobial and hemolytic activities and LPS-neutralizing activity, we designed and synthesized two diastereomers (SMAP-29HD and SMAP-29HDA) with D-amino acid substitution in 19-28 residues of SMAP-29. D-isoleucine and D-allo-isoleucine are substituted in SMAP-29HD and SMAP-29HDA, respectively.

Unlike most of AMPs, some of intracellular-targeting AMPs such as buforin-2, PR-39 and Bac 7 kill bacteria by efficiently crossing cell membrane without inducing severe membrane permeabilization and strongly binding to intracellular nucleic acids [19]. In previous study, we had found that the N-terminal fragment (residues 1-18) of SMAP-29 (called SMAP-18) has intracellular-targeting mechanism. However, it was not clear how SMAP-18 is exerting its activity inside bacterial cytoplasm. Since SMAP-

18 is cationic, it is quite possible that it can binds with negatively charged nucleic acids. At the same time, it is possible that SMAP-18 has other chiral targets inside bacterial cells. Thus, in this study, to examine the stereo-specific interactions, antimicrobial activity and the ability to traverse through the bacterial membrane of D-enantiomer compared to L-enantiomer of intracellular-targeting AMP, we synthesized two enantiomers (SMAP-18D and SMAP-18DA) of SMAP-18 with D-amino acids. D-isoleucine and D-allo-isoleucine are replaced in SMAP-18D and SMAP-29DA, respectively. The sequence and physiochemical properties of the peptides are summarized in Table 1. The molecular weights of the synthetic peptides were verified by MALDI-TOF MS. Table 1 summarizes theoretically calculated and measured molecular weight of each peptide. All peptides had molecular weight values in agreement with their theoretical values, suggesting that the peptides were successfully synthesized.

### 3.2 Hydrophobicity of Peptides

The hydrophobicity of peptides was assessed by measuring the retention time ( $R^t$ ) in analytical RP-HPLC. The retention time of peptides on a reverse-phase matrix was reported to be related to peptide hydrophobicity [26]. The relative hydrophobicity are in the order of SMAP-29D > SMAP-29L > SMAP-29DA > SMAP-29HD > SMAP-29HDA and SMAP-18D > SMAP-18L > SMAP-18DA. The D-enantiomer of SMAP-29 and SMAP-18 showed higher hydrophobicity than their L-enantiomer. SMAP-29DA and SMAP-18DA containing D-all-isoleucine are less hydrophobic than SMAP-29D and SMAP-18D containing D-isoleucine, respectively.

### 3.3 Secondary Structure Studies by CD Spectroscopy

We had examined the CD spectrum of the peptides in sodium phosphate buffer, 30 mM SDS micelles or 0.1% (0.22 mM) LPS (Figure 1). All L-forms (SMAP-29 and SMAP-18) of the peptides have negative peak, while the D-enantiomers (SMAP-29D, SMAP-18D) and D-allo-isoleucine containing Diastereomers (SMAP-29DA, SMAP-18DA) showed positive band, exhibiting a mirror image spectra of L-form. In case of SMAP-29, D-enantiomer (SMAP-29D) showed higher molar ellipticity than its corresponding D-

allo isoleucine-containing diastereomer (SMAP-29DA). However, SMAP-18D and SMAP-18DA showed similar bands with same maxima. Panel A in Figure 1 is the spectra in phosphate buffer, where it shows minima or maxima at 190-200 nm region, which is an indication of random coil structure. SMAP-29HD and SMAP-29HDA did not show any minima at this region. As generally observed in many other AMPs, All L-forms (SMAP-29 and SMAP-18) of the peptides showed a characteristic  $\alpha$ -helical CD spectrum with minima at 208 and 222 nm in the presence of SDS or LPS (panels B and C). D-enantiomers (SMAP-29D and SMAP-18D) and D-diastereomer with D-allo-isoleucine (SMAP-29DA, and SMAP-18DA) showed maxima at these two wavelengths. Interestingly, the SMAP-29HD and SMAP-29HDA peptides showed no specific secondary structure pattern in the presence of SDS or LPS (panels B and C). Their molar ellipticity remains close to zero compared to other SMAP-29 peptides. Curiously, SMAP-29HD and SMAP-29HDA showed a minimum at around 205 nm in presence of LPS (panel C).

### 3.4 Antimicrobial and Hemolytic Activities

Antimicrobial activity of peptides was tested against 3 Gram-negative and 3 Gram-positive bacteria. The results are shown in Table 2. SMAP-29 and its isomeric peptides against six bacterial strains showed relatively strong antimicrobial activity with minimum inhibitory concentration (MIC) within the range of 1-4  $\mu$ M. Overall, SMAP-29L, SMAP-29D and SMAP-29DA showed higher potency against Gram-positive bacteria than Gram-negative bacteria. SMAP-29HD and SMAP-29HDA were equal in their action against both Gram-negative as well as Gram-positive organisms.

Interestingly, SMAP-18D enantiomer and diastereomer (SMAP-18DA) had showed higher potency against all bacteria compared to SMAP-18L. Except *S.aureus*, both SMAP-18D and SMAP-18DA showed fourfold increase in activity against 5 bacterial strains compared to SMAP-18L. All of the peptides displayed potent antimicrobial activity with the MIC range of 4-16  $\mu$ M against three MRSA strains (Table 4). The cytotoxicity of the peptides to mammalian cells was measured by their hemolytic activity towards human red blood cells (hRBCs) (Figure 2, Panel A). Interestingly, SMAP-29DA with D-allo-isoleucine exhibited much less hemolytic activity than SMAP-29L and SMAP-29D. SMAP-29HD and SMAP-29HDA showed



less than 20% hemolysis at the maximum concentration of 256 $\mu$ M. All 3 SMAP-18 peptides did not induce any hemolysis even at 256 $\mu$ M.

### 3.5 Cell Selectivity (therapeutic index)

Cell selectivity is a measure of peptide's capability to differentiate any pathogen against host cells. It is one of the most difficult challenges in the development of antimicrobial agents, especially if the target of action is the cytoplasmic membrane. Cell selectivity of the peptides is expressed as the therapeutic index (TI) =  $HC_{10}/GM$ , where  $HC_{10}$  is peptide concentration needed to reach 10% hemolysis of human red blood cells, while GM is the geometric mean of MICs against six bacterial cells. The TI is a widely accepted parameter to represent the selectivity of antimicrobial agents between bacterial and mammalian cells. Larger values of TI indicate greater cell selectivity. As shown in Table 4, SMAP-29D had a little less TI than SMAP-29L. Interestingly, SMAP-29DA, SMAP-29HD and SMAP-29HDA exhibited a significant increase in TI value by about 3.7-, 12-, 19-fold, respectively, compared to SMAP-29L. SMAP-18D and SMAP-18DA showed 3.6-fold increase in TI compared to SMAP-18L.

### 3.6 Cytotoxicity against RAW264.7 Cells

In addition to hemolytic activity, RAW264.7 macrophage cells were used to evaluate cytotoxicity against mammalian cells. As shown in Figure 2, all of the peptides were non-toxic to RAW264.7 macrophage cells until 5 $\mu$ M. Therefore, LPS-neutralizing activity of the peptides using RAW264.7 cells was conducted at concentration less than 5 $\mu$ M.

### 3.7 Anti-inflammatory Activity

LPS binds to surface TLR-4 molecules, triggering the secretion of various inflammatory factors which contribute to the pathophysiology of septic shock and other immune diseases. To evaluate the anti-inflammatory activity of the peptides, LPS-induced nitric oxide (NO), tumor necrosis factor- $\alpha$  (TNF- $\alpha$ ), interleukin-6 (IL-6) or MCP-1 production was evaluated in macrophage RAW 264.7 cells, in the absence and presence of the peptides by ELISA experiment. As illustrated in Figure 3, LPS induced the secretion of

inflammatory cytokines including NO, TNF- $\alpha$ , IL-6, and MCP-1, which were inhibited by all of the peptides. All of the peptides inhibited TNF- $\alpha$ , IL-6 and MCP-1 production in a dose-dependent manner. This result suggests that these peptides can act as an anti-inflammatory agent. In general, SMAP-29L, SMAP-29D and SMAP-29DA more efficiently inhibited the production of TNF- $\alpha$  from LPS-stimulated RAW 264.7 cells compared to SMAP-29HD and SMAP-29HDA.

### 3.8 Membrane Interaction

The interaction with bacterial membranes is crucial for antimicrobial activity of many AMPs. We had investigated the interaction of peptides with bacterial membranes using two different methods. One method is peptide-induced membrane depolarization. Other method is peptide induced-dye leakage from bacterial membrane-mimicking liposomes. Membrane depolarization was measured by release of the membrane potential-sensitive fluorescent dye diSC<sub>3-5</sub>. This dye is distributed between the cells and medium, depending on the cytoplasmic membrane potential, and self-quenches when concentrated inside bacterial cells. If the membrane is depolarized by the peptide, the dye will be released into the medium, causing a measurable increase in fluorescence. SMAP-29L and its stereoisomers induced a complete membrane depolarization under 2 $\times$ MIC ( $\mu$ M). All of the peptides induced rapid membrane depolarization. SMAP-29HD and SMAP-29HDA took a little more time to reach the maximal membrane depolarization than SMAP-29L, SMAP-29D and SMAP-29DA. On the other hand, SMAP-18L, SMAP-18D and SMAP-18DA caused no or less membrane depolarization. SMAP-18DA caused a small initial rise in fluorescent intensity but it had gradually decreased until the end time of this assay.

The peptide interaction with fluorescent dye-entrapped liposomes is useful to study the peptide-membrane interaction. Highly membrane-active peptides will instantly perturb the membrane and caused sudden release of dye, resulted in the appropriate rise in the measured intensity. To investigate the peptide-membrane interaction, we had treated the peptides with calcein-entrapped bacterial membrane-mimicking liposomes composed of anionic phospholipids. SMAP-29D, SMAP-29DA and SMAP-29L showed rapid dye release indicating a strong action on the membrane (Figure 4, Panel B). As observed in LL-37, the leakage profile of SMAP-29HD and SMAP-29HDA exhibited a

gradual increase in the dye release.

### 3.9 DNA Binding Activity

Although SMAP-18L and SMAP-18D had showed no or less interaction with membranes, SMAP-18D had displayed higher antimicrobial activity against 5 bacterial strains compared to SMAP-18L. Therefore, we examined whether this big difference of antimicrobial activity is due to their DNA binding activity. Peptides were incubated with plasmid DNA and then subjected to agarose gel electrophoresis. As shown in Figure 5, both peptides at 2  $\mu$ M induced the retardation of DNA movement in gel indicating an interaction with DNA

### 3.10 Antimicrobial Activity by Agar Diffusion Assay

In the broth microdilution assay, SMAP-18D showed much higher activity against five bacterial strains compared to SMAP-18L. The antimicrobial effects of the peptides using performing an agar diffusion assay were investigated. The inhibition zone for SMAP-18L was clear but smaller than that of SMAP-18D and SMAP-18DA. On the contrary, the inhibition zone for SMAP-18D and SMAP-18DA was greater, while blurred compared to SMAP-18L (Figure 6).

### 3.11 Time-killing Kinetics

To predict whether AMP is bacteriostatic or bactericidal is difficult using broth microdilution and agar diffusion methods. However, SMAP-18L and SMAP-18D showed a considerable difference in their MIC determined by broth microdilution method and in their inhibition zone observed by agar diffusion method. Therefore, we next investigated the kinetics of time-killing of these peptides against *E.coli*. As shown in Figure 7, SMAP-18L had a smooth gradual curve with a larger negative slope in the first 10 minutes but rate had decreased after that. In case of SMAP-18D, there were an initial drop but a plateau and again slow downward. After 60 minutes, both peptides had showed similar efficacy in terms of number of viable bacteria. SMAP-18L kills *E.coli* rapidly compared to SMAP-18D.

## 4. Discussion

SMAP-29, a highly potent AMP, had initially identified from sheep myeloid cells [27]. It is highly active against board spectrum of pathogens including bacteria, fungi and viruses [10,28]. Besides its potent bactericidal activity, SMAP-29 also showed good LPS-neutralizing activity [12,17,30]. It had been shown that SMAP-29 has two LPS binding sites, residing on either end of peptide, which act cooperatively to bind with LPS [12]. SMAP-29 caused LPS-neutralization and reduction of TNF- $\alpha$  in rat model of sepsis shock [17]. On the other hand, it was also reported that SMAP-29 was not able to inhibit LPS-induced expression of cytokine genes in RAW 264.7 cells, despite having strong LPS binding ability in vitro [31].

The structure of SMAP-29 is having the N-terminal  $\alpha$ -helix, the hinge region of Gly-Pro followed by the hydrophobic segment in the carboxyl terminal region [12]. Like other AMPs, SMAP-29 showed a disordered structure in solution but forms a definite secondary structure at hydrophobic environment [12,13]. SMAP-29 kills bacteria by destabilizing the membrane [13,18]. It was shown that 1-18 residues (termed as SMAP-18) of SMAP-29 is largely retained the antimicrobial activity but significantly reduced the hemolysis [13]. In our previous study, we had found that SMAP-18 differs in its mode of antimicrobial action. SMAP-18 did not destroy the bacterial membrane unlike its parent SMAP-29, but showed bacterial cell-penetrating property. We had also observed that SMAP-18 do not bind with LPS [18]. The target of SMAP-18 inside cytoplasm is not known. For this reason, we have prepared the D-enantiomer (SMAP-18D) and the diastereomer (SMAP-18DA) of L- enantiomer SMAP-18to investigate whether any stereospecific interaction occurs inside cytoplasm. Like other AMPs, the drawbacks of SMAP-29as therapeutic agent are high cytotoxicity, poor protease stability,and less effectiveness at physiological conditions [11,13,31].

Previous study showed that the C-terminal hydrophobic segment of SMAP-29 is responsible for its high hemolytic activity and the N-terminal fragment (SMAP-18) alone did not induce hemolysis. This result prompted us study the hydrophobic interaction of SMAP-29 with lipid bilayer. To know whether stereochemistry of  $\alpha$ -helical AMPs has any role in its membrane interaction, we prepared D-enantiomer of

SMAP-29 comprising D-amino acids (SMAP-29D). We also synthesized the diastereomer (SMAP-29DA), where D-Ile in SMAP-29D is replaced by D-allo-isoleucine. D-allo-isoleucine has smaller retention time compared to L-isoleucine, revealed by N-terminal Edman degradation and subsequent elution of Pin2 peptide [14]. Another study had pointed out that bombinins peptides containing D-allo-isoleucine has higher interaction with membrane compared to corresponding L-form [16].

To obtain SMAP-29 analogs having potent antimicrobial and LPS-neutralizing activities with much less cytotoxicity compared to SMAP-29, we synthesized two diastereomers, SMAP-29HD and SMAP-29HDA, in which 1-18 residues are L-amino acids while 19-28 residues are D-amino acids. The 19-28 residues of SMAP-29HD and SMAP-29HDA are made up of D-isoleucine and D-allo-isoleucine, respectively.

These two diastereomers (SMAP-29HD and SMAP-29HDA) showed much lower hydrophobicity compared to parent SMAP-29 or its enantiomer. This indicates that the total hydrophobicity depends on a continuation of spatial orientation of side chains and on either side of the hinge region (position 18-19) in the parent peptides. SMAP-29HDA showed least hydrophobicity among SMAP-29 peptides indicated that packing of side chains largely contribute to the total hydrophobicity and hydrophobic moments of peptides. It was observed that a little difference (0.4 min) in retention time ( $R^t$ ) of RP-HPLC between SMAP-29L and SMAP-29D. SMAP-29D was slightly more hydrophobic than SMAP-29L (Table 1). Some peptide enantiomers showed same retention time while other enantiomers showed different retention time. Percentage helicity of peptide enantiomers are also varied. [32,33]

CD spectroscopy studies had reported that the D-form peptides containing D-allo-isoleucine has less  $\alpha$ -helicity than the corresponding all L-form peptide [14,15]. Among SMAP-29L, SMAP-29D and SMAP-29DA, SMAP-29DA showed the least  $\alpha$ -helicity in the presence of SDS or LPS (Figure 1). Both SMAP-29HD and SMAP-29HDA did not show any CD spectral character for  $\alpha$ -helical structure in the presence of either SDS or LPS. In CD spectral analysis of L- and D-enantiomers of bovine cathelicidin-derived BMAP-28, these two enantiomers in the presence of TFE showed the mirror plane symmetry [34].

SMAP-29L, SMAP-29D and SMAP-29DA did not show a significant difference in the antimicrobial potency of against all 6 bacteria tested. BMAP-28 has very high

sequence homology with SMAP-29. Also, contains multiple Ile residues (5 Ile) at its C-terminal region. Lynn *et.al.* found that D-enantiomer of BMAP-28 is more active in anti-leishmanial property than L-enantiomer [34], but equally effective on mouse peritoneal model[35]. Won *et.al.* had reported that D-enantiomer had equal antimicrobial potency to L-enantiomer for anoplin AMP [36]. On the other hand, Lee *et.al.* had found that L- to D-amino acids conversion in pleurocidin induced a significant reduction in both antimicrobial and hemolytic activity [37]. SMAP-29HD and SMAP-29HDA showed the MIC range of 2–4  $\mu\text{M}$  against all bacterial strains tested. These two peptides are equal or 2-fold less active compared to SMAP-29.

SMAP-29D is slightly more hemolytic than SMAP-29L. SMAP-29DA showed almost one-half hemolytic activity compared to SMAP-29L and SMAP-29D (Figure 2. Panel A). Both SMAP-29HD and SMAP-29HDA are much less hemolytic than other three SMAP-29 peptides (less than 20% hemolysis at 256  $\mu\text{M}$ ). Kindrachuk *et.al.* had found that D-enantiomer and retro-enantiomer of BMAP-28 are lesser hemolytic than L-enantiomer [34]. However, Chen *et.al.* had reported that D- and L-enantiomer of  $\alpha$ -helical AMP induced same hemolysis on human RBC, which suggest lack of chiral interaction on membrane surface[32].

The antimicrobial activity of SMAP-29L and SMAP-29D are in agreement with the high potency of membrane depolarization and dye leakage (Figure 4). Although SMAP-29HD and SMAP-29HDA are devoid of any definite secondary structure on CD spectrum (Figure 1), these peptides showed antimicrobial activity comparable to that of SMAP-29L and SMAP-29D. Furthermore, these peptides had low levels of hemolytic activity even at very high concentrations. Despite their same sequence, they also had a remarkable reduction in the retention time on RP-HPLC column (Table 1). SMAP-18L, SMAP-18D and SMAP-18DA peptides did not induce hemolysis even at very high concentrations.

The anti-inflammatory activity for SMAP-29 peptides showed similar pattern for inhibition of LPS-induced NO, TNF- $\alpha$ , IL-6. SMAP-29D and SMAP-29DA were more active than SMAP-29L. SMAP-29HD and SMAP-29HDA were slightly less active than other three peptides. Lynn *et.al.* had shown that BMAP-28 and its D-enantiomer and retro-isomer inhibit LPS-induced TNF- $\alpha$  secretion in human PBMC[35]. There is discrepancy in LPS-neutralizing activity of SMAP-29 peptide. Some in vivo

models showed reduction of TNF- $\alpha$ , but some other studies showed no activity for LPS induced cytokine gene expression. It is also shown that SMAP-29 can bind with LPS[17,31].

SMAP-18D enantiomer and SMAP-18DA diastereomer had much higher antimicrobial activity against 5 bacterial strains compared to SMAP-18L enantiomer. SMAP-18L and SMAP-18D had not showed any interaction with intact cells. These peptides displayed the same DNA binding activity (Figure 5). In agar diffusion assay, SMAP-18L exhibited very definite inhibition zone but smaller than that for SMAP-18D and SMAP-18DA. On the contrary, SMAP-18D and SMAP-18DA showed relatively blurred zone with large diameter (Figure 6). In killing kinetics against *E.coli*, SMAP-18L showed a rapid initial bactericidal action compared to SMAP-18D (Figure 7). Our results of killing kinetics and DNA binding activity did not explain why SMAP-18D enantiomer and SMAP-18DA diastereomer have much higher (2-8-fold increase) antimicrobial activity compared to SMAP-18L enantiomer. Further experiments are warranted for membrane translocation efficiency, or other possible targets to elucidate the mechanism for difference in the current observation.

**Table 1.** Amino acid sequences and physicochemical properties of SMAP-29 and SMAP-18 and Enantiomers and diastomers

Peptides	Amino acid sequences	Molecular mass (Da)		Net charge	Retention Time (R <sup>t</sup> ) (min)
		Calculated	Observed <sup>a</sup>		
SMAP-29L	<b>RGLRRLGRKIAHGVKKYGP</b> <b>TVLR</b> <b>II</b> <b>RIA-NH<sub>2</sub></b>	3197.5	3198.9	+10	23.9
SMAP-29D	<b>RGLRRLGRKIAHGVKKYGP</b> <b>TVLR</b> <b>II</b> <b>RIA-NH<sub>2</sub></b>	3197.5	3198.4	+10	24.3
SMAP-29DA	<b>RGLRRLGRKIAHGVKKYGP</b> <b>TVLR</b> <b>II</b> <b>RIA-NH<sub>2</sub></b>	3197.5	3198.5	+10	22.8
SMAP-29HD	<b>RGLRRLGRKIAHGVKKYGP</b> <b>TVLR</b> <b>II</b> <b>RIA-NH<sub>2</sub></b>	3197.5	3198.7	+10	20.9
SMAP-29HDA	<b>RGLRRLGRKIAHGVKKYGP</b> <b>TVLR</b> <b>II</b> <b>RIA-NH<sub>2</sub></b>	3197.5	3198.7	+10	20.6
SMAP-18L	<b>RGLRRLGRKIAHGVKKYG-NH<sub>2</sub></b>	2064.5	2064.8	+8	16.29
SMAP-18D	<b>RGLRRLGRKIAHGVKKYG-NH<sub>2</sub></b>	2064.5	2065.7	+8	16.32
SMAP-18DA	<b>RGLRRLGRKIAHGVKKYG-NH<sub>2</sub></b>	2064.5	2065.8	+8	15.98

<sup>a</sup> Molecular mass were determined using MALDI-TOF-MS.

Black: L-amino acid, Red: D-amino acid, Blue: D-allo-isolucine



**Table 2.** Antimicrobial activity of SMAP-29, SMAP-18, their enantiomers and diastereomers

Peptides	Minimal inhibitory concentration (MIC) <sup>a</sup> (μM)					
	<i>E. coli</i> [KCTC 1682]	<i>P. aeruginosa</i> [KCTC 1637]	<i>S. typhimurium</i> [KCTC 1926]	<i>B. subtilis</i> [KCTC 3068]	<i>S. epidermidis</i> [KCTC 1917]	<i>S. aureus</i> [KCTC 1621]
SMAP-29L	2	4	1	2	2	2
SMAP-29D	4	4	2	2	2	2
SMAP-29DA	2	4	1	2	2	2
SMAP-29HD	4	4	2	4	4	4
SMAP-29HDA	4	4	2	4	4	4
SMAP-18L	16	4	8	32	16	4
SMAP-18D	2	1	2	8	4	4
SMAP-18DA	2	1	2	8	4	4

<sup>a</sup>MIC denotes lowest peptide concentration that causes 100 % inhibition of microbial growth (Three independent measurement with triplicate)

**Table 3.** Antimicrobial activity of the peptides against MRSA

Peptides	Minimal inhibitory concentration (MIC) <sup>a</sup> (μM)		
	MRSA [CCARM 3089]	MRSA [CCARM 3090]	MRSA [CCARM 3095]
SMAP-29L	4	2	2
SMAP-29D	4	4	2
SMAP-29DA	4	4	2
SMAP-29HD	4	4	4
SMAP-29HDA	4	4	4
SMAP-18L	8	16	16
SMAP-18D	8	8	8
SMAP-18DA	8	16	8

<sup>a</sup>denotes lowest peptide concentration that causes 100 % inhibition of microbial growth (Three independent measurement with triplicate)

**Table 4.** Cell specificity (therapeutic index) of SMAP-29, SMAP-18, their enantiomers and diastereomers

Peptides	GM ( $\mu\text{M}$ ) <sup>a</sup>	HC <sub>10</sub> ( $\mu\text{M}$ ) <sup>b</sup>	TI <sup>c</sup> (HC <sub>10</sub> /GM)	Fold <sup>d</sup>
SMAP-29L	2	5.9	2.95	1.00
SMAP-29D	2.5	5.3	2.12	0.72
SMAP-29DA	2	21.5	10.75	3.64
SMAP-29HD	3.5	123	35.14	11.91
SMAP-29HDA	3.5	197	56.2	19.0
SMAP-18L	10.0	256 <	25.6 <	1
SMAP-18D	2.8	256 <	91.43	3.57 <
SMAP-18DA	2.8	256 <	91.43	3.57 <

<sup>a</sup>GM denotes the geometric mean of MIC values from all six bacterial strains.

<sup>b</sup>Peptide concentration ( $\mu\text{M}$ ) for 10% hemolysis in human RBC.

<sup>c</sup>Therapeutic index: the ratio of the HC<sub>10</sub> ( $\mu\text{M}$ ) to the GM ( $\mu\text{M}$ )

<sup>d</sup>The '<' denotes that, within the concentration range tested, there were no HC<sub>10</sub> values to calculate TI, so the reported values were minimal TI calculated with 256  $\mu\text{M}$

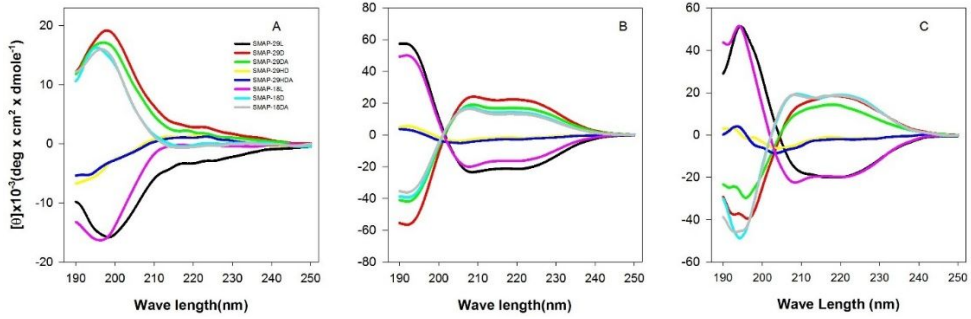


**Figure 1.** Circular dichroism spectra of the peptides in (A) 10 mM sodium phosphate buffer, pH 7.2, (B) 30 mM SDS, 0.1% lipopolysaccharide (c).

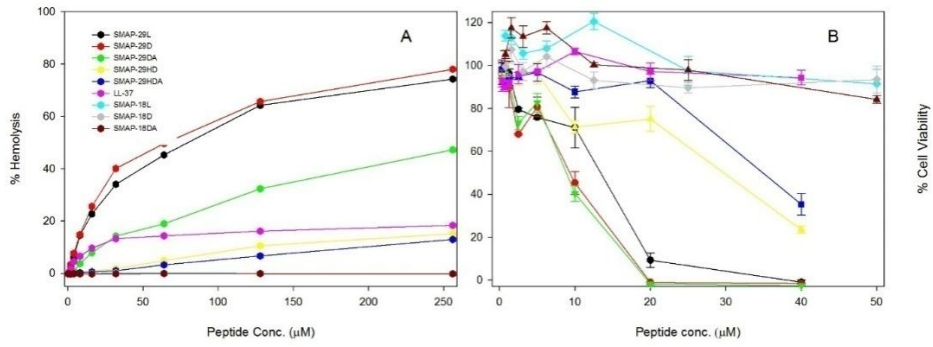


**Figure 2.** Cytotoxicity of Peptides, (A) Peptide induced hemolysis in human RBC (B) Viability of RAW 264.7 cells after Peptide treatment

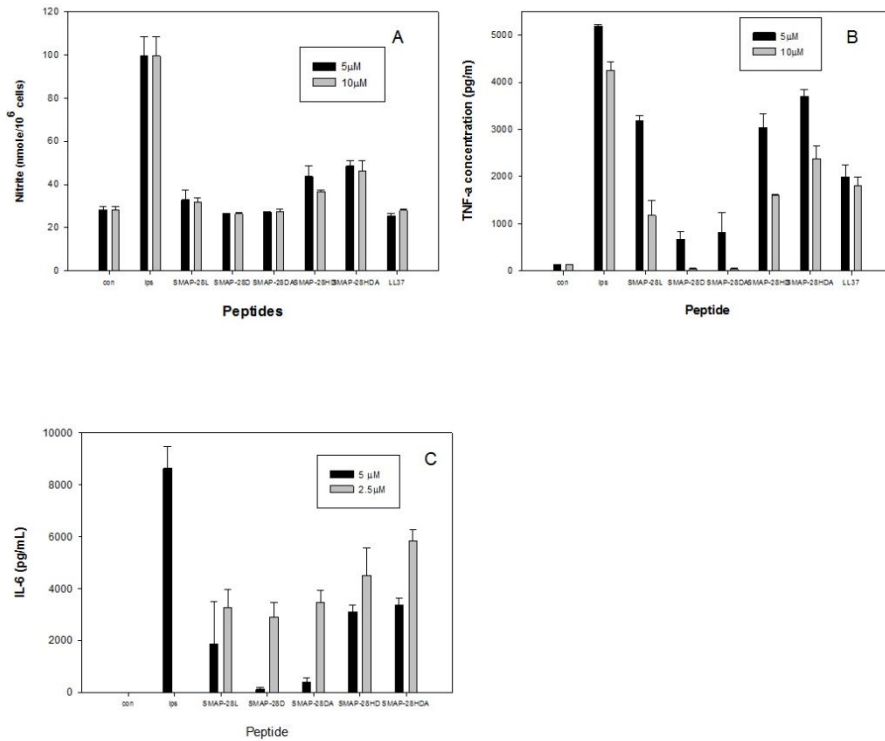


**Figure 3.** Peptide inhibition of LPS induced cytokine induction in RAW 264.7 cells. (A) Nitrate, (B) TNF- $\alpha$ , (C) IL-6, Cells are treated with 20ng of LPS and then treated with corresponding concentration of peptides. B and C were measure using ELISA.

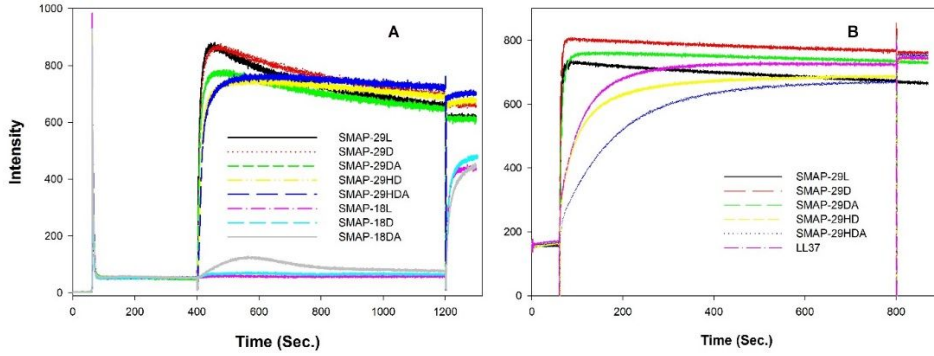


**Figure 4.** Peptide interaction with lipid bilayer. Peptide induced (A) membrane depolarization as measured by release of Disc3 (5) dye from membrane, (B) leak of calcein dye from bacterial membrane mimicking liposomes.

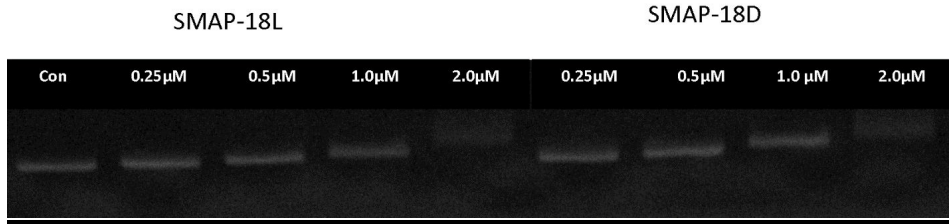


**Figure 5.** SMAP-18L and SMAP-18D – DNA binding affinity: 0.25, 0.5, 1.0, 2.0  $\mu$ M of SMAP-18L and SMAP-18D were treated with 100ng of plasmid DNA. Higher concentrations of peptides caused retardation of DNA band movement. Left to right (control-100 ng DNA only, SMAP-18L, SMAP-18D)



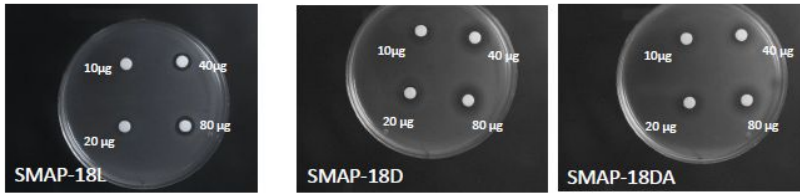


**Figure 6.** MIC against *E. coli* for SMAP-18L, SMAP-18D, SMAP-18DA.

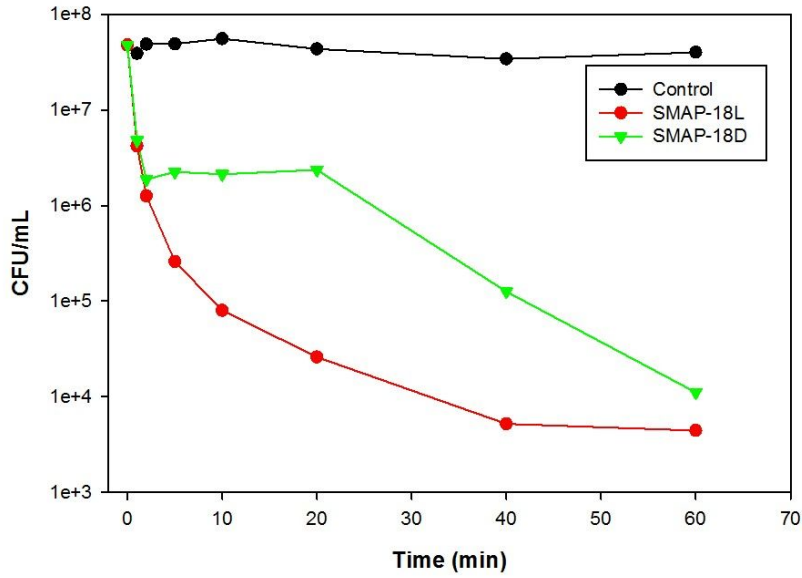


**Figure 7.** Killing Kinetics of SMAP18L and SMAP-18D peptides against *E. coli*

## 5. References

- [1] H. Jenssen, P. Hamill, R.E.W. Hancock, Peptide antimicrobial agents., *Clin. Microbiol. Rev.* 19 (2006) 491–511. doi:10.1128/CMR.00056-05.
- [2] J.L. Fox, Antimicrobial peptides stage a comeback., *Nat. Biotechnol.* 31 (2013) 379–82. doi:10.1038/nbt.2572.
- [3] M.-D. Seo, H.-S. Won, J.-H. Kim, T. Mishig-Ochir, B.-J. Lee, Antimicrobial peptides for therapeutic applications: a review., *Molecules.* 17 (2012) 12276–86. doi:10.3390/molecules171012276.
- [4] K.L. Brown, R.E.W. Hancock, Cationic host defense (antimicrobial) peptides., *Curr. Opin. Immunol.* 18 (2006) 24–30. doi:10.1016/j.coi.2005.11.004.
- [5] A. Peschel, H.-G. Sahl, The co-evolution of host cationic antimicrobial peptides and microbial resistance., *Nat. Rev. Microbiol.* 4 (2006) 529–36. doi:10.1038/nrmicro1441.
- [6] Y. Rosenfeld, N. Papo, Y. Shai, Endotoxin (lipopolysaccharide) neutralization by innate immunity host-defense peptides. Peptide properties and plausible modes of action., *J. Biol. Chem.* 281 (2006) 1636–43. doi:10.1074/jbc.M504327200.
- [7] M. Marta Guarna, R. Coulson, E. Rubinchik, Anti-inflammatory activity of cationic peptides: application to the treatment of acne vulgaris., *FEMS Microbiol. Lett.* 257 (2006) 1–6. doi:10.1111/j.1574-6968.2006.00156.x.
- [8] R.E.. Hancock, G. Diamond, The role of cationic antimicrobial peptides in innate host defences, *Trends Microbiol.* 8 (2000) 402–410. doi:10.1016/S0966-842X(00)01823-0.
- [9] R.E.W. Hancock, H.-G. Sahl, Antimicrobial and host-defense peptides as new anti-infective therapeutic strategies., *Nat. Biotechnol.* 24 (2006) 1551–7. doi:10.1038/nbt1267.
- [10] R.M. Dawson, C.-Q. Liu, Cathelicidin peptide SMAP-29: comprehensive review of its properties and potential as a novel class of antibiotics, *Drug Dev. Res.* 70 (2009) 481–498. doi:10.1002/ddr.20329.

- [11] B. Skerlavaj, M. Benincasa, A. Risso, M. Zanetti, R. Gennaro, SMAP-29: a potent antibacterial and antifungal peptide from sheep leukocytes, *FEBS Lett.* 463 (1999) 58–62. doi:10.1016/S0014-5793(99)01600-2.
- [12] B.F. Tack, M. V Sawai, W.R. Kearney, A.D. Robertson, M.A. Sherman, W. Wang, et al., SMAP-29 has two LPS-binding sites and a central hinge., *Eur. J. Biochem.* 269 (2002) 1181–9. doi:10.1046/j.0014-2956.2002.02751.x.
- [13] S.Y. Shin, E.J. Park, S.T. Yang, H.J. Jung, S.H. Eom, W.K. Song, et al., Structure-activity analysis of SMAP-29, a sheep leukocytes-derived antimicrobial peptide., *Biochem. Biophys. Res. Commun.* 285 (2001) 1046–51. doi:10.1006/bbrc.2001.5280.
- [14] G. Carmona, A. Rodriguez, D. Juarez, G. Corzo, E. Villegas, Improved protease stability of the antimicrobial peptide Pin2 substituted with D-amino acids., *Protein J.* 32 (2013) 456–66. doi:10.1007/s10930-013-9505-2.
- [15] M.L. Mangoni, N. Papo, J.M. Saugar, D. Barra, Y. Shai, M. Simmaco, et al., Effect of natural L- to D-amino acid conversion on the organization, membrane binding, and biological function of the antimicrobial peptides bombinins H., *Biochemistry.* 45 (2006) 4266–76. doi:10.1021/bi052150y.
- [16] C. Coccia, A.C. Rinaldi, V. Luca, D. Barra, A. Bozzi, A. Di Giulio, et al., Membrane interaction and antibacterial properties of two mildly cationic peptide diastereomers, bombinins H2 and H4, isolated from *Bombina* skin., *Eur. Biophys. J.* 40 (2011) 577–88. doi:10.1007/s00249-011-0681-8.
- [17] A. Giacometti, O. Cirioni, R. Ghiselli, F. Mocchegiani, G. D’Amato, R. Circo, et al., Cathelicidin peptide sheep myeloid antimicrobial peptide-29 prevents endotoxin-induced mortality in rat models of septic shock., *Am. J. Respir. Crit. Care Med.* 169 (2004) 187–94. doi:10.1164/rccm.200307-971OC.
- [18] B. Jacob, Y. Kim, J.-K. Hyun, I.-S. Park, J.-K. Bang, S.Y. Shin, Bacterial killing mechanism of sheep myeloid antimicrobial peptide-18 (SMAP-18) and its Trp-substituted analog with improved cell selectivity and reduced mammalian cell toxicity., *Amino Acids.* 46 (2014) 187–98. doi:10.1007/s00726-013-1616-8.
- [19] Y. Lan, Y. Ye, J. Kozłowska, J.K.W. Lam, A.F. Drake, A.J. Mason, Structural contributions to the intracellular targeting strategies of antimicrobial peptides., *Biochim. Biophys. Acta.* 1798 (2010) 1934–43. doi:10.1016/j.bbamem.2010.07.003.

- [20] K.H. Park, Y.H. Nan, Y. Park, J. Il Kim, I.-S. Park, K.-S. Hahm, et al., Cell specificity, anti-inflammatory activity, and plausible bactericidal mechanism of designed Trp-rich model antimicrobial peptides., *Biochim. Biophys. Acta.* 1788 (2009) 1193–203. doi:10.1016/j.bbame.2009.02.020.
- [21] M. Stark, L.-P. Liu, C.M. Deber, Cationic hydrophobic peptides with antimicrobial activity., *Antimicrob. Agents Chemother.* 46 (2002) 3585–90.
- [22] D.A. Scudiero, R.H. Shoemaker, K.D. Paull, A. Monks, S. Tierney, T.H. Nofziger, et al., Evaluation of a soluble tetrazolium/formazan assay for cell growth and drug sensitivity in culture using human and other tumor cell lines., *Cancer Res.* 48 (1988) 4827–33.
- [23] M. Wu, E. Maier, R. Benz, R.E. Hancock, Mechanism of interaction of different classes of cationic antimicrobial peptides with planar bilayers and with the cytoplasmic membrane of *Escherichia coli.*, *Biochemistry.* 38 (1999) 7235–42. doi:10.1021/bi9826299.
- [24] C.L. Friedrich, D. Moyles, T.J. Beveridge, R.E. Hancock, Antibacterial action of structurally diverse cationic peptides on gram-positive bacteria., *Antimicrob. Agents Chemother.* 44 (2000) 2086–92.
- [25] J.-J. Koh, S. Qiu, H. Zou, R. Lakshminarayanan, J. Li, X. Zhou, et al., Rapid bactericidal action of alpha-mangostin against MRSA as an outcome of membrane targeting., *Biochim. Biophys. Acta.* 1828 (2013) 834–44. doi:10.1016/j.bbame.2012.09.004.
- [26] T. Baczek, R. Kaliszan, Predictions of peptides' retention times in reversed-phase liquid chromatography as a new supportive tool to improve protein identification in proteomics., *Proteomics.* 9 (2009) 835–47. doi:10.1002/pmic.200800544.
- [27] L. Bagella, M. Scocchi, M. Zanetti, cDNA sequences of three sheep myeloid cathelicidins, *FEBS Lett.* 376 (1995) 225–228.
- [28] M. Benincasa, M. Scocchi, S. Pacor, A. Tossi, D. Nobili, G. Basaglia, et al., Fungicidal activity of five cathelicidin peptides against clinically isolated yeasts., *J. Antimicrob. Chemother.* 58 (2006) 950–9. doi:10.1093/jac/dkl382.
- [29] K.A. Brogden, V.C. Kalfã, M.R. Ackermann, D.E. Palmquist, P.B. McCray, B.F. Tack, The ovine cathelicidin SMAP29 kills ovine respiratory pathogens in vitro

- and in an ovine model of pulmonary infection., *Antimicrob. Agents Chemother.* 45 (2001) 331–4. doi:10.1128/AAC.45.1.331-334.2001.
- [30] Y. Sang, M. Teresa Ortega, K. Rune, W. Xiau, G. Zhang, J.L. Soulages, et al., Canine cathelicidin (K9CATH): gene cloning, expression, and biochemical activity of a novel pro-myeloid antimicrobial peptide., *Dev. Comp. Immunol.* 31 (2007) 1278–96. doi:10.1016/j.dci.2007.03.007.
- [31] Y. Xiao, Y. Cai, Y.R. Bommineni, S.C. Fernando, O. Prakash, S.E. Gilliland, et al., Identification and functional characterization of three chicken cathelicidins with potent antimicrobial activity., *J. Biol. Chem.* 281 (2006) 2858–67. doi:10.1074/jbc.M507180200.
- [32] Y. Chen, A.I. Vasil, L. Rehaume, C.T. Mant, J.L. Burns, M.L. Vasil, et al., Comparison of biophysical and biologic properties of alpha-helical enantiomeric antimicrobial peptides., *Chem. Biol. Drug Des.* 67 (2006) 162–73. doi:10.1111/j.1747-0285.2006.00349.x.
- [33] Y.-H. Nan, B.-J. Lee, S.-Y. Shin, Prokaryotic Selectivity, Anti-endotoxic Activity and Protease Stability of Diastereomeric and Enantiomeric Analogs of Human Antimicrobial Peptide LL-37, *Bull. Korean Chem. Soc.* 33 (2012) 2883–2889. doi:10.5012/bkcs.2012.33.9.2883.
- [34] J. Kindrachuk, E. Scruten, S. Attah-Poku, K. Bell, A. Potter, L. a Babiuk, et al., Stability, toxicity, and biological activity of host defense peptide BMAP28 and its inversed and retro-inversed isomers., *Biopolymers.* 96 (2011) 14–24. doi:10.1002/bip.21441.
- [35] M.A. Lynn, J. Kindrachuk, A.K. Marr, H. Jenssen, N. Panté, M.R. Elliott, et al., Effect of BMAP-28 antimicrobial peptides on *Leishmania major* promastigote and amastigote growth: role of leishmanolysin in parasite survival., *PLoS Negl. Trop. Dis.* 5 (2011) e1141. doi:10.1371/journal.pntd.0001141.
- [36] A. Won, M. Khan, S. Gustin, A. Akpawu, D. Seebun, T.J. Avis, et al., Investigating the effects of L- to D-amino acid substitution and deamidation on the activity and membrane interactions of antimicrobial peptide anoplin., *Biochim. Biophys. Acta.* 1808 (2011) 1592–600. doi:10.1016/j.bbamem.2010.11.010.
- [37] J. Lee, D.G. Lee, Structure-antimicrobial activity relationship between pleurocidin and its enantiomer., *Exp. Mol. Med.* 40 (2008) 370–6. doi:10.3858/emm.2008.40.4.370.

## Acknowledgement

I would like to express my sincere gratitude to my adviser Prof. Song Yub Shin, who has been a great mentor for me. He had encouraged, supported, cared, and guided me throughout my PhD study and research. Besides professional training, true to a great mentor, he had imparted me with wisdom that I can take to the rest of my life. It was a great opportunity to get trained in Prof. Shin's lab, and I am thankful to him for all the experience and knowledge I have received from him. I would also like to thank rest of my thesis committee members, Prof. Park, Prof. Choi, Prof. SH Lee and Prof. CW Lee for their insightful comments and suggestions.

It was my beloved wife Remya's support made it possible for me to reach here. I am greatly indebted to her for allowing me to continue and finish my PhD. Her consistent support and encouragement helped me to overcome the tough times in life. I am thankful to my parents for nurturing my aptitude, and they always granted me the liberty to pursue my interests. Though it is beyond words, I would like to appreciate and thank my family for all the help and sacrifices they had committed to shape my life. Huge thanks to Kunjechi, Pinchi, Aliyan, and Eapen for their care and support during all these years.

A special thanks to Dr. Gopal and Imam, for all those countless tea breaks packed with witty, interesting chats about anything 'under and beyond the sun'. Apart from those refreshing moments, they had helped me personally and professionally wherever required. I am greatly thankful to Sung Il-Jo for being my good friend and for his language helps, especially during the first year of my PhD life.

I am thankful to Dr. Nan for he had given me the technical training during my first year. Big thanks to Raja, who made the day to day lab life alive and fruitful in multiple ways, for patiently listening to all my blabbering and for various help to perform my experiments. Thanks to Miss. Seon, for she had prepared some peptides and reagents for my research. I am grateful to Dr. CK Lee, and Dr. Park their help and trouble shooting of the machines and equipments.

Many thanks to 'team crazy bikers' for those magnificent weekend cycling trips through the countryside. Cheers and thanks to all friends, especially, Balaji, Anand and Pavithra for giving many cherishing memories of friendship.

## Dedication

Dedicated to Remya, and to my Parents, for their encouragement and support.